SELF-CALIBRATING CRICKET MOTES FOR INDOOR NAVIGATION

A thesis submitted in partial fulfillment

of the requirements for the degree of

Master of Science in Engineering

By

YOGENDRA J. PATIL

B. E., Maharashtra Institute of Technology, India, 2007

2011

Wright State University

WRIGHT STATE UNIVERSITY

SCHOOL OF GRADUATE STUDIES

June 09, 2011

I HEREBY RECOMMEND THAT THE THESIS PREPARED UNDER MY SUPERVISION BY YOGENDRA JAYANT PATIL ENTITLED Self-calibrating Cricket Motes for Indoor Navigation BE ACCEPTED IN PARTIAL FULFILLMENT OF THE REQUIREMENTS FOR THE DEGREE OF Master of Science in Engineering.

Kuldip Rattan, Ph. D.
Thesis Director

Kefu Xue, Ph. D.
Chair, Department of Electrical Engineering

Committee on
Final Examination

Kuldip Rattan, Ph.D.

Marian Kazimierczuk, Ph.D.

Xiaodong Zhang, Ph.D.

Andrew Hsu, Ph.D.
Dean, School of Graduate Studies

Abstract

Patil, Yogendra. M.S.Egr., Department of Electrical Engineering, Wright State University, 2011.Self-calibrating Crikcet Motes for Indoor Navigation.

Global Positioning System (GPS) plays a vital role for providing localization to the autonomous robots. But the quality of the GPS signal degrades in an indoor location and hence GPS cannot be used for indoor localization. Cricket motes are location-aware system that can provide localization service to its users in an indoor location. Cricket motes apply the acoustic ranging technique to find distance between two points. But before a user can use this localization system, assigning coordinate system to the motes requires manual assistance. This project presents a novel algorithm for self-calibration of the cricket motes to a coordinate system when positioned around a rectangular field. The initial localization of the cricket motes is performed using the trilateration technique so as to get a rough estimate of their position. Then, the logic of Simultaneous Localization and Mapping (SLAM) algorithm is applied to obtain positioning accuracy within 5 cm.

Contents

List of Figures

1 Introduction

In the field of robotic research, navigation of autonomous robotic system is an essential topic. In order to achieve navigation of an autonomous robot from one point to other, it is essential to provide the robot with its location information at every instance. Providing the robot with its location information allows the robot to know where it is, so that it can navigate towards destination. Navigation of an autonomous robot is considered an important issue in manufacturing industries, where an Automated Guided Vehicle (AGV) needs its location information at every instance [26].

Automated Guided Vehicle (AGV) is a mobile robot that autonomously navigates itself towards required location by following markers or wires, or using information obtained from laser scanners. For wired sensor navigation, wires are placed approximately 1 inch below the ground surface, which emits radio frequency signals [26]. The sensors attached to the bottom of the AGV detect the transmitted radio frequency signals from the wire, and follows it [26]. For guided tapes navigation, tapes (magnetic or colored) are placed along the route to be followed by the AGV. The AGV is fitted with the appropriate sensor, which detects the tapes placed on the ground and navigates towards required location. For laser target navigation the AGV is equipped with a laser scanner. As the AGV moves, it scans the local area and updates its own location information constantly. Using the knowledge of it's (constantly updated) location information, the AGV can navigate itself towards destination. Similar, to wired sensors, guided tapes, laser target navigation, cricket motes can be used to provide location information to AGV or autonomous robots [26].

Cricket motes are low-cost, low-power operated indoor location-aware system that can also provide localization service to its user. Cricket system uses the method of trilateration to provide localization service to its users. According to the method of trilateration, it is necessary that every cricket mote should be assigned with its

coordinate position. Cricket motes cannot self-calibrate themselves to a coordinate system. Therefore, before a user can use the localization service of the cricket system, assigning coordinates to the cricket motes has to be done manually [19].

1.1 Motivation And Goal of this thesis

Though cricket motes can provide localization service to its user, the user needs to configure the cricket motes to a coordinate system. Assigning coordinate points to the cricket motes can prove tedious in situations where large number of cricket motes are used. In such situations, it is better to use self-calibrating cricket motes, which are capable of configuring themselves to a local coordinate system and later on can provide pin-point localization to it's users. Applications where an autonomous robot (like the AVG) requires the knowledge of its pin-point location, these self-calibrating cricket motes can be considered as useful solution. The main objective of this thesis work is concentrated on devising an algorithm for self-calibration of cricket motes. Once these cricket motes calibrate themselves to a coordinate system, they can provide localization to its users.

P Bodhi et al. [17] formulated a technique for localization of a group of stationary cricket motes using a mobile cricket mote. This technique is referred to as mobile assisted localization (MAL), because the user carrying a cricket mote needs to move from place-to-place to assign coordinate points to the stationary cricket motes. In MAL technique, distance measurements are obtained between the mobile cricket mote and the stationary cricket motes. The recorded distance measurements results in a set of equations, which allows to find the unknown location (coordinate points) of each stationary cricket motes. This technique requires assistance from a mobile device to obtain the distance measurements at suitable points. After collecting the distance measurements, the coordinate assignment to the stationary cricket motes is obtained on the mobile device. This technique can prove tedious when large number of cricket

motes are used for providing localization service to its users. P Bodhi et al. [18] proposed another technique called as Anchor Free Localization (AFL), in which the algorithm arbitrarily assigns coordinates to all motes based on the connectivity information of the motes and not on the actual distance information. Then the error values for distance measurements are calculated, which is the difference between the actual measured distance values (obtained using MAL technique) and the distance computed (using the knowledge of arbitrarily assigned coordinates). These error values are then optimized for the minimal sum-of-square error for all edges. The final objective is to achieve the coordinate assignment until the error reaches zero. This technique uses MAL technique, which requires a person or a mobile device in initial stages to obtain inter-cricket mote distances. It is based on trial-and-error procedures which results in calculation overhead. Also the noisy measurements can cause large amount of error in co-ordinate assignment. D Moore et al. [19] formulated a new algorithm to overcome the error in coordinate assignment caused by the noisy distance measurements. In this method a set of four nodes which qualify a given criteria, form a *robust quadrilateral*. Interconnecting these *robust quadrilateral* results in a robust graph. Thus this method can tolerate the noisy measurements and coordinate assignment to the motes can be easily obatined with good level of accuracy. But, in case of low node connectivity, the nodes cannot form the *robust quadrilateral* and algorithm fails.

Although the above techniques provide great engineering ingenuity and effectiveness to assign coordinates to the nodes, some of them either require manual assistance or are limited up to certain range (less than 1 m). This thesis deals with developing a novel algorithm for the self-calibration of the cricket motes to a coordinate system. In this thesis, the cricket motes are mounted on a stand and arranged in such a fashion that they can communicate with each other and can obtain inter-mote distance mea-

surements. Using the inter-mote distance knowledge the cricket motes can calibrate themselves to a coordinate system. In order to understand the communication range and accuracy level in distance calculation, various experiments are conducted. The error in localization due to faulty distance measurements is reduced by the logic of the Simultaneous Localization And Mapping (SLAM) algorithm.

1.2 Common Terminologies

In this thesis the terms cricket motes, localization and accuracy zone will be encountered several times. These words mean different in different fields. Hence, as a first step it is essential to define their meaning with respect to this thesis work.

1.2.1 Cricket motes

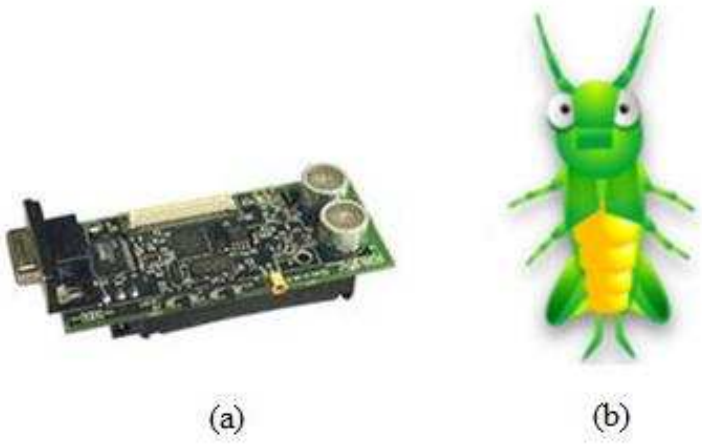

Figure 1: (a)Cricket mote and (b)Cricket insect.

The central component of this thesis work is the cricket mote. These devices are capable of obtaining distance measurement between two points. In order to understand the reason for referring this device as cricket mote, consider first the word

cricket. Similar to the insect cricket, cricket mote emits sound periodically. Only the difference is that, cricket insect emits sound of audible frequency range, while cricket mote emits an ultrasonic pulse. The basic definition for the word mote is *a very small particle*. In the field of wireless sensor networks, the wireless sensor device is usually referred by the term mote, because of its small size. A cricket mote is a wireless sensor device, available in the size of 10 cm$\times$ 4 cm$\times$ 3 cm ($length \times breadth \times depth$).

1.2.2 Localization

The basic definition for localization is *to restrict* (*something*)*to a particular location or area*. In mathematical terms localization is referred as *the mathematical process of providing meaningful location information to a given point*. In relation to this thesis, providing x and y coordinates to a cricket mote or a point is referred as localization.

1.2.3 Accuracy zone

The term accuracy zone will be encountered very often in chapters 3 and 4. Accuracy zone is defined as the region in which the cricket mote has the highest level of accuracy in the distance estimation as compared to other points.

1.3 Organization of this Thesis

In summary, Chapter 2 discusses about the various available localization systems and the reason for choosing cricket motes over other localization systems. In Chapter 3, the behavior of the ultrasonic sensors of the cricket mote is discussed in detail. Data obtained from various field experiments is provided so as to understand the accuracy level and the communication range of a cricket mote. Chapter 4 provides a detail step-by-step formulation for the proposed algorithm based on the obtained experimental field data. Chapter 5 discusses about the experimental simulation results obtained by implementing the algorithm in MATLAB. Chapter 6 discusses about the final conclusions observed in this thesis work and the future scope.

2 Literature Review

The main objective of this thesis is to find a novel algorithm for self-calibration of the cricket motes. After the self-calibration of the cricket motes to a local coordinate system, these motes can provide localization service and can also be used for navigation purpose of autonomous robots. This chapter presents a brief detail for various localization systems available and their underlying technique for localization. Considering the benefits provided, the cricket location-aware system is used in this thesis work over other localization systems.

Section 2.1 describes the Global Positioning System and some of its limitations. Section 2.2 provides a general detail to various indoor localization systems and outlines some of their limitations. Section 2.3 introduces to the cricket location-aware systems. The distance estimation technique used by the cricket mote is discussed in detail in section 2.4. Section 2.5 discusses about the trilateration technique applied by the cricket motes for localization of a point. Section 2.6 provides a brief detail to localization technique using law-of-cosines and the advantages provided by trilateration over law-of-cosine technique is discussed in section 2.7. Some of the limitations for trilateration technique are discussed in section 2.8. Section 2.9 introduces to the logic of SLAM algorithm. The Kalman Filtering and the Extended Kalman Filtering technique is described in section 2.10 and 2.11 respectively.

2.1 Global Positioning System (GPS)

Throughout ages one of the important topics considered is to find an easy solution for determining one's location or to navigate oneself towards destination, when encountered with an unknown environment. Various means and technology have been used to simplify this task but were accompanied with major disadvantages. Methods like landmarks (works only in local area and may change depending upon time),

navigation using celestial bodies (available only during night time), LORAN (LOng RAnge Navigation system have limited coverage area and easy to jam), OMEGA (radio-navigation system used by US Navy for military aviation users only, had low precision and subjected to radio interference) were widely used before the advent of the Global Positioning System (GPS)[2][4].

The Global Positioning System (GPS) was introduced by the U.S. Department of Defense (DoD) for navigation and positioning purpose with high precision than the previous systems. NAVSTAR (NAVigation System using Timing And Ranging) satellites (manufactured by Rockwell International that cost around $12 billion) are a network of 24 satellites (+7 spare in reserve) orbiting earth at distance of 12,000 miles. Each satellite has an orbital period of 11 hours and 58 minutes and is installed with highly accurate atomic clocks operating at fundamental frequency of 10.23MHz. These twenty-four satellites orbit in six orbital planes or paths with each orbit consisting of four satellites [4].

Each GPS satellite is assigned a "Pseudo Random Code" (PRC) which is transmitted on a radio frequency carrier signal. The PRC is a long complicated sequence of zeros and ones, and appears like a random electrical noise. As each GPS satellite orbits around the earth, it periodically transmits radio frequency signals (containing PRC) to the surface of the earth. The GPS receiver (usually referred as user segment) computes the time difference between the GPS transmitted and received signal to obtain the distance between the satellite and the receiver. The following section summarizes the steps involved in calculating the distance between the GPS satellite and the receiver [2][4].

2.1.1 Distance estimation by GPS

The simplest way to determine the distance travelled by an entity between any two points is to multiply the speed of the entity with the difference in time value t_1

(recorded at the starting point) and time value t_2 (recorded after the arrival of the entity at the end point).

$$distance = speed \times time - difference(t_2 - t_1) \quad (1)$$

Therefore, to estimate the distance between the GPS satellite and the GPS receiver, the time-difference factor given by equation (1) should be first calculated. Assume that the GPS satellite and receiver are generating the PRC's at the same time. The GPS satellite transmits the generated PRC code on a radio frequency carrier wave to the surface of the earth. Even though the radio frequency signal travel at the speed of light, it takes some time for the satellite transmitted signal to reach the surface of the earth. Thus GPS receiver receives a delayed version of the PRC from the GPS satellite. Therefore, in order to run the PRC generated by the receiver in synchronization with the received PRC from the GPS satellite, the PRC of the receiver should be shifted back or delayed by some amount of time. This time shift corresponds to the time difference factor given by equation (1). Multiplying the calculated time difference factor with the speed of light, the distance between the satellite and the receiver can be easily calculated [2][4].

With the distance measurements calculated from at least four GPS satellites; the receiver can then calculate its position (latitude, longitude and altitude) by using the method of trilateration [2]. Calculating four distance measurements not only pin-points the location of the user but also helps the receiver with universal time synchronization [4].

2.1.2 Universal time-synchronization by GPS receiver

With one distance measurement obtained from a satellite, the position of the receiver is narrowed down to a surface of the sphere. The receiver may lie anywhere on this sphere, with radius equal to calculated distance measurement and center as the satel-

lite. Two distance measurement gives rise to two spheres, which when intersect gives rise to a circle. The receiver may lie anywhere on this circle. Introducing a third distance measurement narrows down the position of the receiver to two different points. Using only three distance measurements, one could easily find the actual point (position of the receiver), because one of the two points is always way off from the surface of the earth. A fourth satellite distance measurement not only narrows down the position of the receiver to a single point but also helps it in time synchronization [4]. To understand this concept, assume that the GPS receivers are equipped with perfectly synchronized atomic clocks (which cost around $50K to $100K) like the GPS satellites. Due to perfect time synchronization between GPS satellites and receiver all the four distance measurements will accurately intersect at a single point. Since, the GPS receivers are not equipped with atomic clocks; imperfect time-synchronization with the satellites atomic clocks will always cause the fourth sphere to intersect the previous three spheres at some other points. This gives an indication to the receiver that it is not synchronized with the universal time and needs a single correction factor. The receiver calculates a single correction factor and subtracts it from all its four distance measurements, causing the spheres to intersect at a single point. This is how the receiver synchronizes its time with the universal time using four distance measurements calculated from four different satellites [4].

Once the position of the user is determined, other factors like speed, journey progress can be easily obtained. Hence, GPS is the most widely used technology for pin-point localization as compared to other localization systems [4].

Though GPS provides localization with precision, following factors should be considered which degrade the quality of the GPS.

1. **Number of Visible Satellites**

   There should be at least four visible GPS satellites for the GPS receiver to

calculate its exact location. Without four satellites above the horizon and no universal time synchronized clock in the receiver, the calculated position of the user will always be way-off from the actual position [4]. Due to dense vegetation and large building structures, it is difficult to receive the GPS satellite signals constantly. Factors like electro-magnetic interference, multi-path fading, lack of line-of-sight is commonly observed in urban areas, which affect the reception of the GPS satellite signals [2].

2. **Selective Availability**

   Though GPS is made available for common people, its service is discontinued during the state of national emergency. During this time the GPS always provide faulty measurements to the user, resulting in incorrect localization. So, all types of applications using the GPS service are considered useless [4].

3. **Sources of Error in GPS**

   Table 1 summarizes sources of error in GPS that are unavoidable. The table has been directly obtained from source [2]. It should be noted that these values are not constant, but are subject to variances.

Serial No.	Sources of Errors	Amount of Errors
1	Satellite Clocks	1.5 m to 3.6 m
2	Orbital errors	less than 1 m
3	Ionosphere	5 m to 7 m
4	Troposhere	0.5 m to 0.7 m
5	Receiver Noise	0.3 m to 1.5 m
6	Multipath Fading	0.6 m to 1.2 m

Table 1: Sources of Error in GPS [2].

The errors described in Table 1 can be reduced using a differential GPS. But this in-turn increases the cost of the receiver unit and also makes it bulky [5].

Though the factors described in Table 1 affect the GPS performance to greater extent, one of the most important and main factor to be considered is the unavailability of the GPS satellite signals inside a building structure. In indoor locations, GPS signals are often degraded by multi-path interference and hence are not suitable for providing localization. Hence GPS satellite signals are not suitable for providing indoor localization.

2.2 Indoor Localization Systems

As most of the day-to-day activities are in indoor environments, indoor location-aware systems are in great demand today. Indoor applications such as navigation through the building or tunnel, real-time tracking, health care monitoring can be easily achieved using indoor location-aware systems [10].

Consider some of the following indoor localization and tracking systems that have been developed over the years for indoor use.

1. **Sonitor Tags and Receivers**

   These are Real Time Location Systems (RTLS) developed by Sonitor Technologies. In this system, tags attached to the devices or users transmit a unique ultrasonic identification signal. The ultrasonic identification signal is then received by strategically mounted ultrasonic detectors on walls. These detectors further pass on the message via a wired or wireless LAN to a central computer. The central computer then computes and passes on the user's location information to the devices (like PC's, PDA, portable cellular phones) connected to the network. These devices have good room level accuracy and are energy efficient. But accuracy fails for room with larger size. The system requires centralized administration and user privacy is not maintained. It also requires devices that support LAN connections. The set-up or the deployment of the system is complicated and cost involved is high [6].

2. **Ubisense**

   Ubisense RTLS uses ultra-wideband (UWB) radio signals, which results in more accuracy than other RTLS technologies (which simply uses radio signals). UWB radio signals are more resistant to multi-path interference as compared to normal radio signals. "Also it uses a combined technique of Angle of Arrival (AoA) and Time Difference of Arrival (TDoA) together with filter-based location algorithms" [7]. Thus the system is more robust in environments which are prone to multi-path radio propagation and precision obtained in localizing the user is high. Accuracy obtained is tens of centimeters and these devices have an ability to cover larger areas. Though these devices have high localization precision, cost involved is high [7].

3. **Firefly Motion Tracking System**

   Firefly Motion Tracking System is designed to track the motion of a moving object. This system basically consists of a bunch of infrared (IR) LED tags along with cables and a tag controller attached to the device or human body. The measurement system consists of three charge-coupled device (CCD) cameras, which helps in determining the 3D-position of each IR LED tags using image processing techniques. Though this system provides 3D-position along with orientation and accuracy of 3 mm, it is mostly restricted to a single user. Also, cost of set up is high and the system consists of wired tags which limits the user motion and movements to some extent [8].

4. **Active Badge**

   Active Badge is considered to be the pioneer of indoor localization systems. In this system, a tag (called as Active Badge) emits a unique signal every 15 seconds. Network of IR sensors, located strategically, pick up the tag emitted signal information (Received Signal Strength, RSS information) and then

forward it to the central system for processing. The central station processes the available information and then sends to its clients, which displays this information in a useful visual form. Though the architecture of this system is simple, Active Badges have difficulty in determining location-information for places where large numbers of fluorescent lighting or direct sunlight is present, as these sources of light generate spurious infrared emissions [9]. Thus accuracy rate is greatly affected in such situations. Weight factor is another problem, because the tags (Active Badge) that need to be carried by the user weigh around 40 grams [9] [10].

5. **Active Bat**

   The Active Bat localization system was developed by AT&T technologies to provide better performance than Active Badge. Users carry a hand-held device or a tag, called as Active Bat. The tags emit an ultrasonic pulse, on request by the main controller of the system, to a grid of ceiling-mounted receivers. At the same time the main controller sends a (radio frequency) reset signal to the ceiling-mounted receivers [9]. Each ceiling mounted receiver then calculates the difference between the radio frequency reset signal and the ultrasonic signal emitted by the tag. The local controller then sends this information to a main controller, which then performs the position calculation of the user [9]. Active Bats have the ability to cover larger areas and can also be used for 3D positioning. To increase accuracy, the system requires large number of ceiling-mounted sensors, which in-turn increases the cost of the overall system. Centralized administration is required for the operation of Active Bat localization systems [9].

6. **RADAR**

   Developed by Microsoft systems research group, RADAR is an indoor tracking

system based on IEEE 802.11 WaveLAN wireless networking technology. At the base station, RADAR computes the received signal strength and signal-to-noise ratio of the signals emitted by the wireless (user) devices and then uses this data to calculate the 2D position of the devices within a given room. This system requires few base stations and can use the existing WLAN infrastructure. As each object being tracked by this system must support a wireless LAN, it is impossible to use this system for small power-limited devices. Accuracy level available with this system is low [9].

Therefore, it would be easier to deploy an indoor-localization system which takes into account factors like preservation of user privacy, decentralized administration (to avoid administration and management overheads), user friendly set-up, cost effective, low power operated, small in size, multi-user (many users using the same network at a time). The Cricket Localization system provides all these major advantages [11][12].

2.3 Cricket Location-Aware System

Cricket motes are location-support system or location-aware system developed at Computer Science and Artificial Lab (CSAIL), MIT for providing indoor localization to its user. The main purpose of the Cricket motes is to provide user with its space location and not pin-point localization in a given space. Cricket motes are available in the size of 10 cm$\times$ 4 cm$\times$ 3 cm ($length \times breadth \times depth$). They operate at a voltage value of 3 V (2 AA batteries) and have a life-span of 4 weeks. Cricket motes cost around $20 non-commercially [12][13]. The following data provided is directly obtained from P Bodhi, PhD dissertation 2005.

1. **US Transmitter**: The US Transmitter sub-module "drives a 40 kHz piezo-electric open-air US transmitter at 12V" which generates US pulses of duration 125 μs [12].

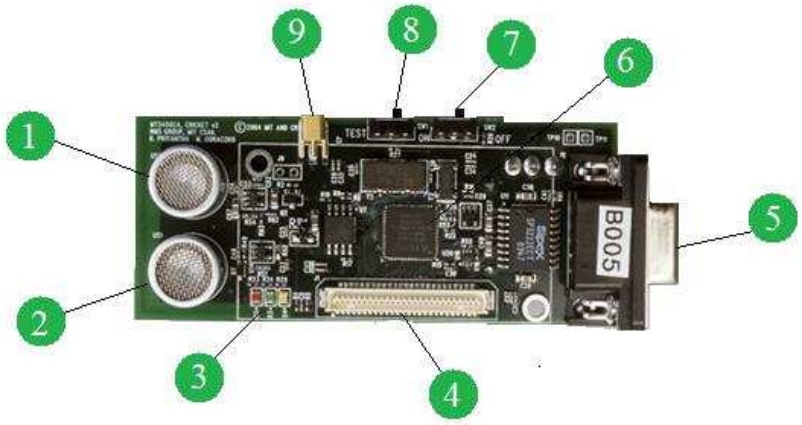

Figure 2: The Cricket mote.

2. **US Receiver**:This sub-module uses an "open-air type piezo-electric transducer operating at 40 kHz" to detect US signals. The output of this transducer is connected to a "two-stage programmable voltage gain", which detects the US signal only when the amplifier output goes above a preset threshold level [12].

3. **Diagnostic LEDs**:The three LEDs are used for diagnosing or signaling a mote problem during operation of the system (similar to that of wireless sensor networks) [12].

4. **Expansion Connector**:This is a "51-pin expansion connector used by the cricket mote which can be connected to other compatible Mica motes". It is also used to burn the firmware on to the cricket motes using a MIB 510 programming board [13].

5. **Serial Port Connector**: The RS 232 connector or the serial port interface provides connection of the cricket motes to PC or to a PDA for mutual communication[12].

6. **Microcontroller**:Cricket uses "ATMEL MEGA 128L" microcontroller operating at 7.3728 MHz in active mode and 32.768 kHz in sleep mode". This sub-module is a"8-bit processor with 8 kB of RAM memory, 128 kB of FLASH ROM and 4 kB of EEPROM". The micro-controller operates on "3 V and draws about 8 mA current in active stage" [12].

7. **Power Switch**: This switch is used for turning the cricket mote ON or OFF [13].

8. **Test Switch**: This switch is used when the cricket mote runs in beacon mode. In beacon mode, switching to 'ON' position disables the onboard RS 232 chip, which in turn saves power [12].

9. **Radio Antenna connector**: The external radio antenna connector is used in case an external radio transceiver is needed to achieve higher range capability for cricket motes [12].

Cricket mote consists of CC1000RF radio transceiver (not shown in figure) which operates at 433 MHz and is designed to receive and transmit data at 19.2 kilobits/s [12].

Figure 3 shows the standard set-up for the cricket location-aware system. Three cricket motes are attached to the ceiling and are pre-configured with coordinate points. The user usually carries a single cricket mote, attached to a device. The location of the user is calculated on the device, to which the listener is attached. To provide the localization service, the cricket motes operates in two modes-

1. **Beacon Mode**: In beacon (US transmitter) mode the cricket mote periodically transmits the US pulse and a RF signal. The RF signal contains information about the mote, e.g. its space ID, co-ordinate, ON time, etc. Beacons are usually mounted on the ceilings and are pre-configured with coordinate values

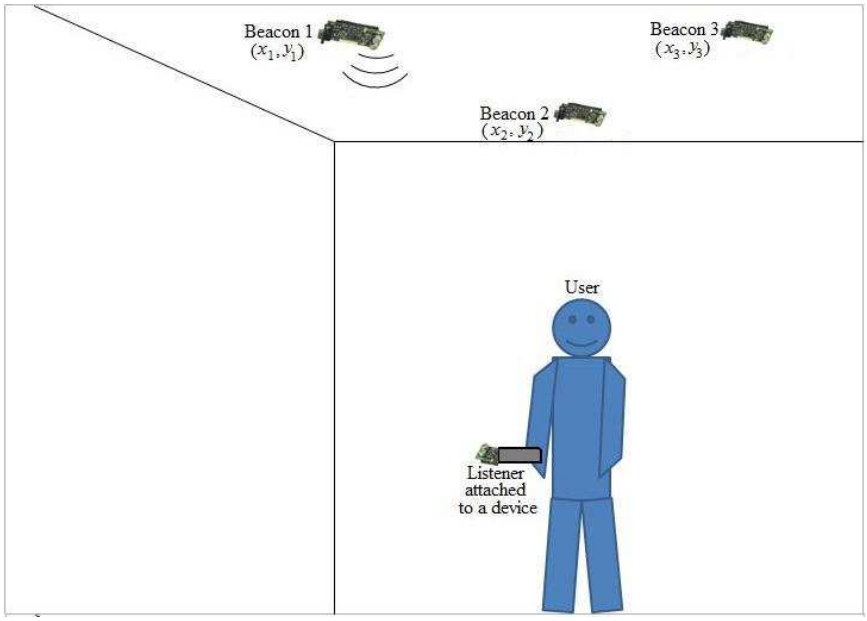

Figure 3: Beacons attached to the ceiling and listener connected to the user device.

assigned by the user [12]. For simplicity cricket mote in beacon mode will be directly referred to as beacon.

2. **Listener Mode**: In listener (US receiver) mode the cricket mote receives the US pulse transmitted by the beacon. Listeners are usually connected to PCs or any system requiring location support. The calculation of the listener's position (coordinate assignment) is usually done by the PC or the system to which the listener is connected [12]. For simplicity cricket mote in listener mode will be directly referred to as listener.

Cricket system applies the Time Difference of Arrival (TDoA) and the trilateration techniques together to determine the unknown position of the listener or user carrying listener [11] [12].

2.4 Time Difference of Arrival (TDoA)

In order to maintain simple hardware and cost effectiveness, Cricket employs an easy technique called as Time Difference of Arrival (TDoA) to calculate the distance between any two points [12].

In beacon mode, cricket mote transmits a radio frequency (RF) signal and an ultrasonic (US) pulse simultaneously. RF signal travels at the speed of light (3×10^8 m/s), while US signals travel at the speed of sound (344 m/s). Thus, when the beacon transmits a RF signal and a US signal, RF signal reaches the listener end instantaneously while US signal takes some time to arrive. The listener is programmed to record the time of the RF signal arrival and the time of the US signal arrival. The difference of the two recorded time instances gives the time difference factor as stated in equation (1). Multiplying this factor with the speed of sound gives the distance measurement or the separation between the beacon and the listener [11][12].

Figure (4)shows the TDoA technique applied by the cricket motes to calculate the

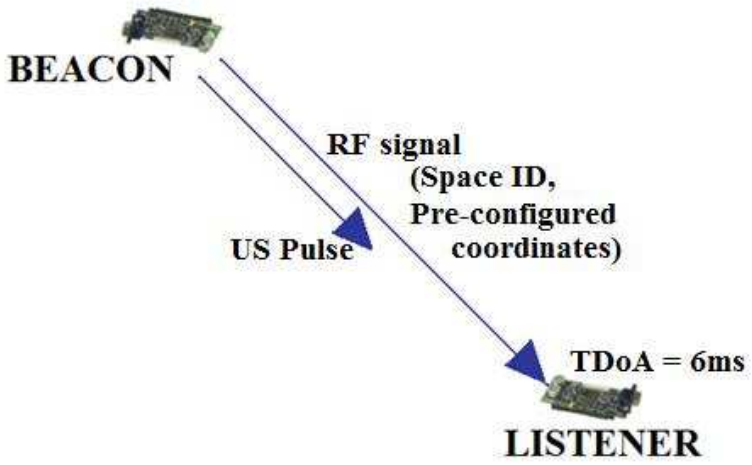

Figure 4: TDOA technique used in Cricket motes.

distance separation between two points. Cricket in beacon mode transmits an ultrasonic chirp or pulse and a radio signal at the same time. The transmitted radio signal contains the beacon space ID and its coordinates [12][13]. As the speed of the RF signal (V_{RF}) is much greater than the speed of US signal (V_{US}) the time of arrival of the two signals at the listener end is different. The listener records the time of arrival of RF signal (T_{RF}) and US signal (T_{US}) and calculate the time difference (ΔT) in arrival as,

$$\Delta T = T_{US} - T_{RF} \tag{2}$$

The distance (d_{LB}) between the listener and the beacon is calculated as,

$$\Delta T = \left(\frac{d_{LB}}{V_{US}}\right) - \left(\frac{d_{LB}}{V_{RF}}\right) \tag{3}$$

$$= \frac{d_{LB}(V_{RF} - V_{US})}{V_{RF} \cdot V_{US}} \tag{4}$$

As the velocity of RF signal is much greater than that of the US signal, i.e. $V_{RF} >> V_{US}$.

$$\Delta T = d_{LB} \cdot \frac{V_{RF}}{V_{RF} \cdot V_{US}} \tag{5}$$

$$= \frac{d_{LB}}{V_{US}} \tag{6}$$

$$d_{LB} = \Delta T \cdot V_{US} \tag{7}$$

Therefore, the listener needs to simply calculate the time difference in arrival of the RF and US signals and multiply it by the velocity of the US signal to get the distance measurement of the listener from a particular beacon [12][13].

For example, if the time difference in arrival of the two signals $\Delta T = 0.006$ s and speed of sound $V_{US} = 34400$ cm/s, then the value of d_{LB} is given by,

$$d_{LB} = 0.006s \times 34400cm/s = 206.4cm \tag{8}$$

Although the speed of the US signals alters with the changes in surrounding atmospheric conditions, cricket mote is equipped with temperature sensors to estimate the surrounding temperature value [12].

Cricket system uses acoustics technology for ranging purposes. The main drawback faced by the acoustics ranging techniques is the requirement of line-of-sight between the transmitter and the receiver. If there is an obstacle between the transmitter and the receiver, then the US signal is not received. Ranging technologies using only RF signals do not suffer from this drawback [13]. RF ranging technology usually uses one of the following two approaches for distance measurements-

1. **Received Signal Strength (RSS)**: As the name suggests in RSS method, the amplitude or strength of the received RF signal is calculated at the receiver end. "A mathematical model is assumed for the RF signal path loss up to the receiver end" [13]. By adding appropriate quantities (which depend on the ambient conditions) to the RSS mathematical model, the distance separation between the transmitter and receiver can be obtained by measuring the received signal strength. As, the path loss model is highly dependent on the surrounding environmental factors, deriving such a complicated mathematical model is not an easy task. "System which uses only single frequency RF signal will be more susceptible to multi-path fading which will result in substantial error in the distance estimation" [13]. "Thus by using multi-frequency and filtering techniques the above problem can be overcome" [13]. But, this in turn increases the cost of the system. Also, most of the time, the transmitted power is a function of the battery voltage of the transmitter. Thus, without the knowledge of the original transmitted power, it may not be possible to correctly estimate the path loss [13].

2. **Time of Flight (ToF)**: In this second ranging technique, the time of flight

or arrival of the radio signal alone is measured and multiplied by the speed of light. This technique is more precise than RSS technique but has two major setbacks-

- It requires highly synchronized clocks to calculate the arrival time of the signal which travels at the speed of light. Even a mistake in calculating $1/6^{th}$ of the second can cause a large error value in the distance calculations [13].
- To achieve higher accuracy, the system requires clocks which tend to be expensive in terms of both power and cost. GPS satellites use atomic clocks which cost around $50K$ to $100K$ (per clock) and are constantly monitored for achieving accurate timing [2] [4] [13].

Considering issues like power consumption, cost of overall system, small size, easy to use; systems employing acoustics techniques proves to be more beneficial and accurate than other ranging technologies. Only issues for acoustics ranging systems like distance coverage and requirement of line-of-sight still remains unanswered.

2.5 Trilateration

Cricket mote applies the technique of trilateration to calculate the unknown position of the listener using the knowledge of three known measurements (three coordinates and distances) [12]. Figure (5) shows the technique used in trilateration method to estimate the unknown location (coordinate) of a point by using three known measurements [14]. As shown in Figure (5), location of points A, B and C are known, i.e. A(x_a, y_a), B(x_b, y_b) and C(x_c, y_c) while that of point X (x, y) is unknown. The distance measurements from point A, B and C to point X are known. Let the distance from point A to X be d_{AX}, from point B to X be d_{BX} and from point C to X be d_{CX}. The distance between X and A can be determined using the Euclidean distance

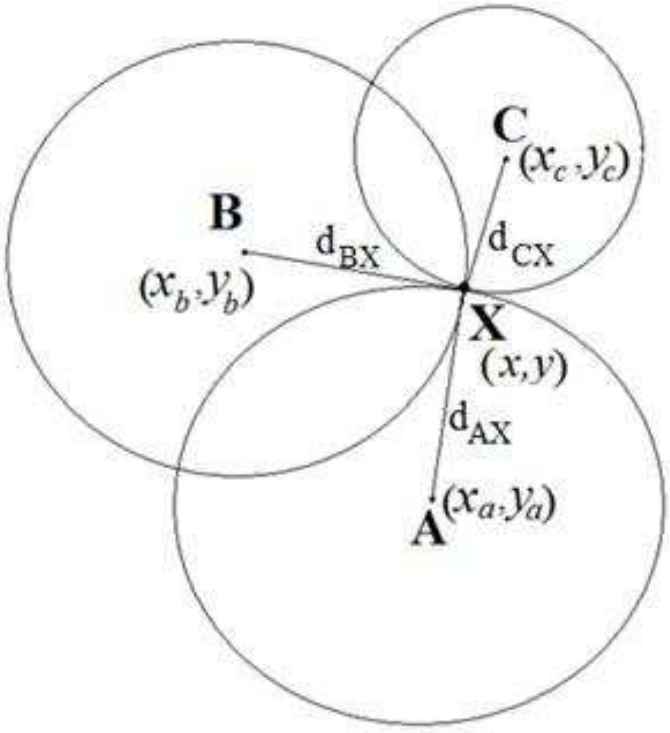

Figure 5: Trilateration technique.

formula as,

$$(x - x_a)^2 + (y - y_a)^2 = (d_{AX})^2 \tag{9}$$

Similarly, the distance between X and B, X and C is given by,

$$(x - x_b)^2 + (y - y_b)^2 = (d_{BX})^2 \tag{10}$$

$$(x - x_c)^2 + (y - y_c)^2 = (d_{CX})^2 \tag{11}$$

Equations(9),(10) and(11)give rise to three circles. As shown in figure 6 (a), equation (9) gives rise to a circle centered at A (x_a, y_a) with radius equal to d_{AX}. The point X with unknown location may lie anywhere on this circle.

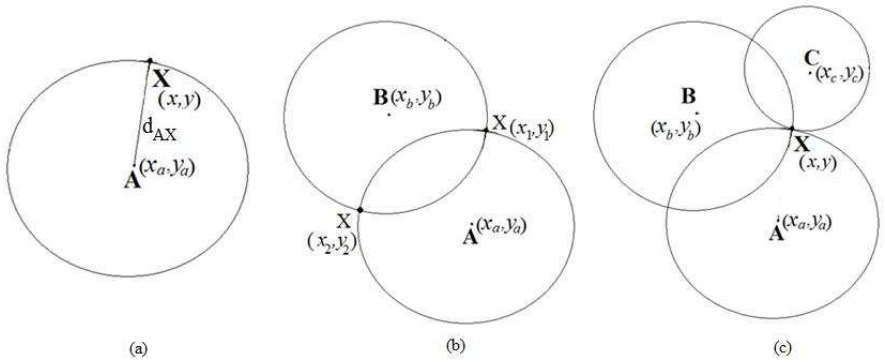

Figure 6: Localization process in 2D space using trilateration technique.

Figure 6 (b) depicts the scenario when equations (9) and (10) are solved simultaneously. This gives rise to two possible set of solution, viz. $(x_1,\ y_1)$ and $(x_2,\ y_2)$. Therefore, point X may lie at point $(x_1,\ y_1)$ or at $(x_2,\ y_2)$. This ambiguity can be eliminated by using equation (11). Solving equations (9), (10) and (11) simultaneously gives rise to a unique solution for the position of the point X as $(x,\ y)$ (Figure 6). Thus for a 2D space, if the distances from three points of known position to a point with unknown position are known; then the point with unknown location can be uniquely located [15].

2.6 Law of Cosines

Another technique to calculate the unknown position of a point is by using law of cosines. In this technique if the distance measurements between the origin, a point on Y-axis and the point of unknown location are known; then the point with its position unknown can be localized [21].

Figure 7 shows the point C with its position $(x_c,\ y_c)$ unknown. Point A(0, 0) is the origin of the coordinate system and point B lies on the Y-axis with coordinates $(0,\ c)$. For ΔABC, the distance between point A and B equal to c, between point B and C equal to a and between point C and A equal to b. The values of a, b and c are

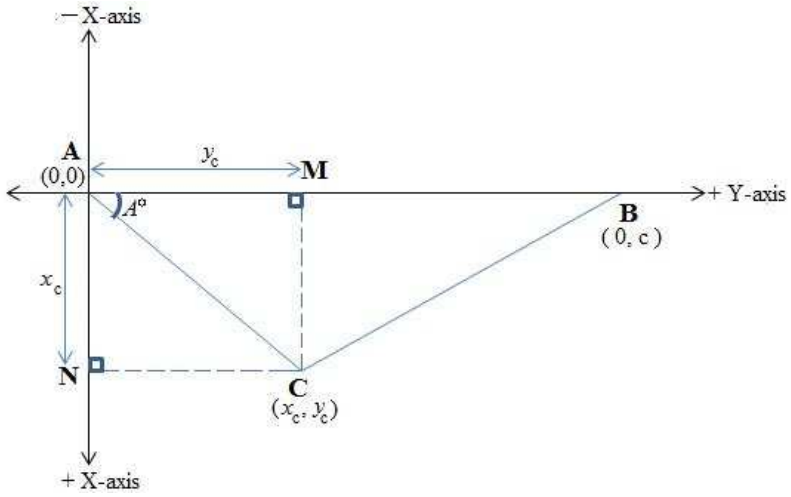

Figure 7: Localization using Law of Cosine technique.

known quantities.

Therefore, l(AB)=c, l(BC)=a and l(AC)=b. Using trigonometric laws for ΔAMC,

$$x_c = l(AC) \cdot \sin(A) = b \cdot \sin(A) \tag{12}$$

$$y_c = l(AC) \cdot \cos(A) = b \cdot \cos(A) \tag{13}$$

To find the unknown angle A, Pythagoras theorem is applied to ΔCMB,

$$l(CB)^2 = l(MB)^2 + l(CM)^2 \tag{14}$$

$$a^2 = (c - y_c)^2 + x_c^2 \tag{15}$$

$$a^2 = c^2 - 2 \cdot c \cdot y_c + y_c^2 + x_c^2 \tag{16}$$

Equating values of x_c and y_c from equation(12)and (13) in equation (16),

$$a^2 = c^2 - 2 \cdot c \cdot (b \cdot \cos(A)) + b^2 \cdot \cos^2(A) + b^2 \cdot \sin^2(A) \tag{17}$$

$$a^2 = c^2 - 2 \cdot c \cdot b \cdot \cos(A) + b^2 \cdot (\cos^2(A) + \sin^2(A)) \tag{18}$$

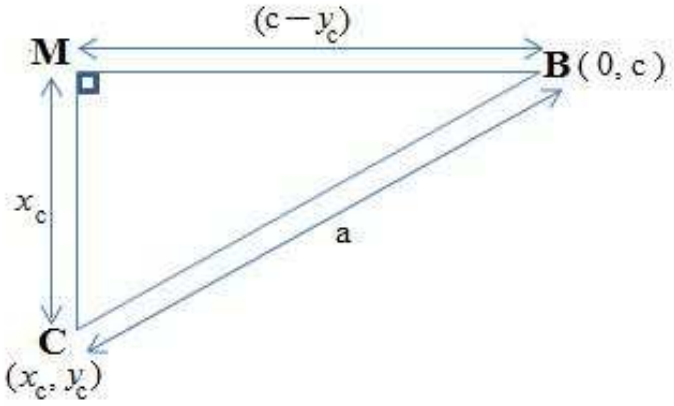

Figure 8: ΔCMB, with its edges.

$$a^2 = c^2 - 2 \cdot b \cdot c \cdot \cos(A) + b^2 \tag{19}$$

Rearranging all terms in equation(19)

$$2 \cdot b \cdot c \cdot \cos(A) = b^2 + c^2 - a^2 \tag{20}$$

$$\cos(A) = \left(\frac{b^2 + c^2 - a^2}{2 \cdot b \cdot c} \right) \tag{21}$$

$$A = \arccos \left(\frac{b^2 + c^2 - a^2}{2 \cdot b \cdot c} \right) \tag{22}$$

Substituting the value of angle A calculated by equation (22) in equations (12) and (13) the unknown position of point C can be easily calculated [21].

2.7 Advantages of trilateration techniques

In order to calculate the unknown coordinate using the law of cosine technique, distance measurements from the origin and a point on Y-axis to the point of unknown location should be known. In case of wireless sensor networks, if a sensor node (of unknown position and limited communication range) is not able to calculate its distance

from the sensor node (assigned as the origin), then the coordinate assignment to the node with unknown position cannot be achieved and the law-of-cosine technique fails in such situation.

Figure 9 shows two points P and P′, having same distance measurements from

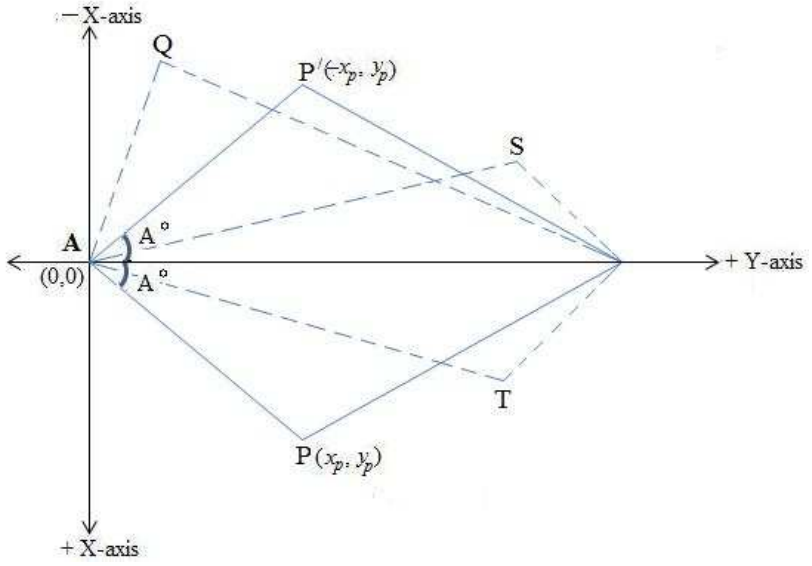

Figure 9: Ambiguity in localization of point due to law of cosines.

points A and B and are to be localized using law of cosines technique. Using equations(12),(13) and(22) the unknown position of point P yields as (x_p, y_p) and that of point P′ yields as (x_p, y_p). But point P′ lies on the negative side of X-axis and therefore its actual position is $(-x_p, y_p)$. Therefore, there is an ambiguity in localizing a point's position using the law of cosine technique. Similar case is observed in localizing points Q, S and T where there is an ambiguity in deciding which side of the X-axis these points lay.

Unlike law-of-cosine technique, any point localized using the method of trilateration results in the true position of the point, provided that the distance measurements are accurate.

In order to localize a given set of points P, Q, R, S, T, U, V distributed in 2D space

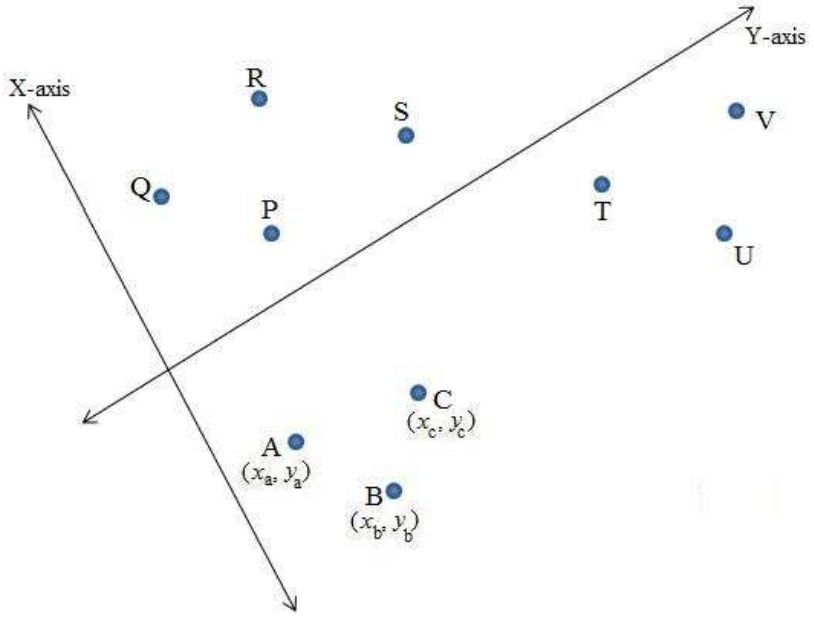

Figure 10: Localization of set of points using trilateration.

as shown in figure 10; the localization of these points obtained using the trilateration technique results in the actual location of the point. For example, position of points A, B, C are known and is given by (x_a, y_a), (x_b, y_b), (x_c, y_c) respectively. In general the points with known location (here A, B, C) may or may not be located at the origin or on the Y-axis. The distance measurements from points A, B, C to points of unknown position P, Q, S, are known. By using the method of trilateration, the points P, Q, S can be easily localize. Now, if the distance measurements from the previously localized points P, Q, S to the points R and T are known, then points R and T can be localized easily. Thus, the final mapping of all the points obtained in this manner results in the actual localization (true position) of the points [15][18].

2.8 Limitations of trilateration techniques

Though trilateration results in actual localization of a given point, the two factors that contribute in the accuracy for the final localization are-

1. **Geometric Layout of the points**: The level of accuracy on the final localization of a point depends on the geometric layout of the points. To understand this concept, consider the graphical interpretation for the trilateration method. In order to localize a point using the method of trilateration, the point of intersection of three circles is considered as the actual location of the point; where the centers of the three circles are the points with known location (or coordinates). But it should be noted that the three points must be non-collinear or else the intersection of the three circles is observed at two possible points. This gives rise to two possible solutions for the position of the point with unknown location. Figure 11 shows the condition when the three collinear points are

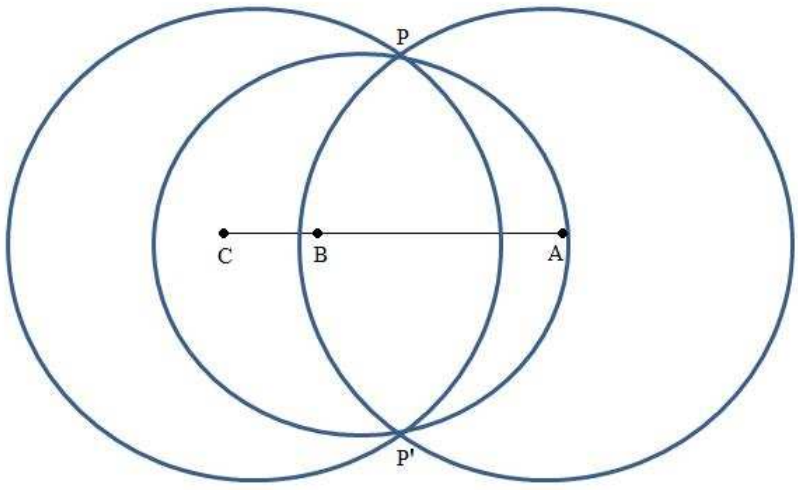

Figure 11: Ambiguity in localization of point P due to three collinear points A, B, C.

used to localize a point in 2D space. Points A, B, C are the collinear points

with known location and point P is to be localized using the method of trilateration. As shown in figure 11 the three circles intersect at two points viz. P and P′, which represents the two possible solutions for the point P. Thus the three collinear points A, B, C represents a bad geometric layout and there is an ambiguity in localizing a point P. As shown in figure 12, when the point B

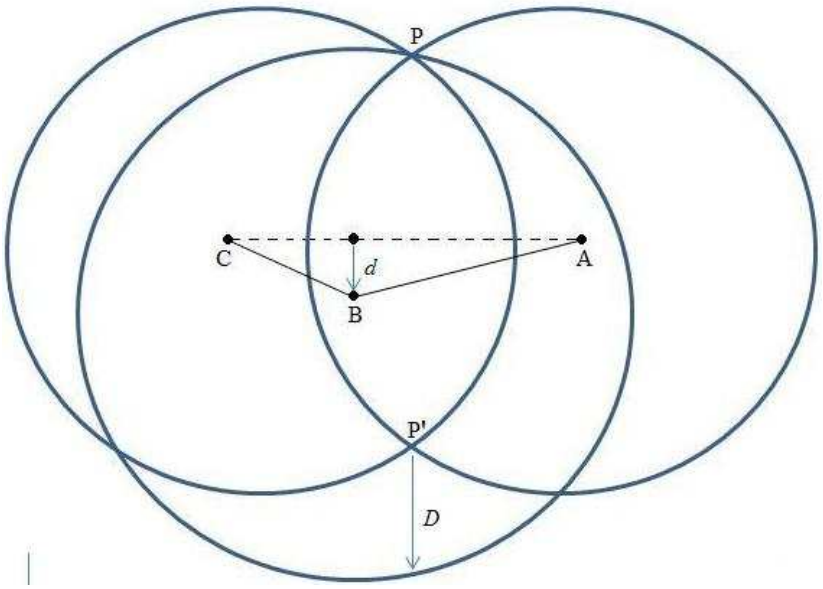

Figure 12: Unique localization of point P due to three non-collinear points A, B, C.

is moved downwards by a distance d, correspondingly the circle with center as B is moved away from point P′ by distance D which is equal to 2d. Due to this the three circles intersect at point P only, and the point P is uniquely localized using the method of trilateration. Thus the three non-collinear points A, B, C represents a good geometry layout and the point P is localized uniquely.

Unlike point B, the geometric layout for points A and C do not play a significant role in localizing point P (point with unknown location). In case when the three points A, B, C are non-collinear, even if the distance between the points A and

C is increased or decreased along the line passing through A and C; circles with centers as A and C still intersect at two points viz. P and P′ as shown in Figure 12. Hence, it really does not matter where the two points A and C are located along the line passing through A and C.

2. **Accuracy in distance measurements**: The method of trilateration results in the actual localization of the points only if the distance measurements obtained are accurate. But in real world applications accurate distance measurements can never be obtained, because no ranging instruments are perfect and have some inaccuracies and uncertainty due to inherent noise. Due to this problem, the localization of the points is in-accurate and the final graph formed due to this localization highly differs from the actual graph representation. The solution to this problem is obtained by simply applying the Simultaneous Localization And Mapping (SLAM) algorithm [22][23].

2.9 Simultaneous Localization And Mapping (SLAM) algorithm

SLAM algorithm is widely used in the field of autonomous robot navigation, especially in scenarios where a robot encounters an unknown environment with its own location unknown. Using the SLAM algorithm technique, the robot builds a map of an unknown location, while at the same time localizes itself for a given current location [22]. The SLAM algorithm consists of the following components-

1. **Robot**: In order to implement the SLAM algorithm, a mobile robot equipped with ranging device, is necessary. The mobile robots may be wheeled or legged such as humanoid robots, an autonomous underwater vehicles or an autonomous planes [23].

2. **Dead Reckoning**: The mobile robots discussed above should have dead reck-

oning ability. Dead Reckoning is the process of estimating one's current position based upon the knowledge of previously determined position. For example, the dead reckoning for a wheeled robot can be defined as estimating the robots position just from the rotation of the wheels. It should be noted that in this method as the current position is determined based on the robot's previous position, the error in position calculation increases as the robot's journey progresses. Hence, the method is sensitive to errors and requires rapid and accurate data collection, accurate sensor calibration and processing [23].

3. **Ranging Device**: The ranging device usually used by the mobile robot is a laser scanner to estimate its position from certain landmarks. Landmarks for a given environment can be defined as the features which are usually immobile, re-observable and can be easily distinguished from the environment, e.g. a landmark in a room can be considered a chair, table, door, etc. Sonars are used by the underwater vehicles as ranging device, because of its effectiveness as compared to laser scanners [23].

4. **Extended Kalman Filtering**: In SLAM algorithm, the robot uses a ranging device along with the dead reckoning technique to locates it's own position. Even though the ranging device has a high level of accuracy; some inaccuracies are still present, as no real world instruments are prefect. Due to this imperfectness in the ranging device, the localization of the robot and the landmarks has errors. The Extended Kalman Filtering (EKF) technique is used in SLAM algorithm to get a good estimate for the position of the robot and the landmarks by combining the knowledge of the dead reckoning and ranging device measurements [23][24].

5. **Data Association**: One of the crucial step in SLAM algorithm is the data as-

sociation. In order to get a good estimate of the robot's position, it is necessary to re-observe the landmark several times, until the uncertainty in the robots position is reduced. Initially, when the robot observes a landmark it gathers information (usually referred to as data features) about the landmark. When the robot re-observes the previously seen landmark to estimate its own position, the robot makes sure that the observed landmark is similar to its previously seen landmark. Therefore the robot associates the data features of the re-observed landmark to its previously observed data features. This is usually referred to as the data association phase. This assures the robot that it is not wrongly associating an observed landmark to the previously seen landmarks. If the robot wrongly associates the landmarks, then the robot will wrongly build the map of the environment and the SLAM algorithm fails in this case. The robot maintains a database, to store the landmarks and it associated data features [23].

In the following explanation of the SLAM algorithm, the robot used has an ability to estimate its position using dead reckoning and is also equipped with ranging devices that can calculate the robots distance from a landmark [24].

Figure 13 shows the logic for implementing the SLAM algorithm. At instant I1, the robot's position is given by (x, y, θ), which is considered as the robot's initial state. The robot chooses some landmarks and calculates its distance from the landmark using the ranging devices. As shown in figure 13, at instant I1 the robot chooses Landmark 1, Landmark 2 and Landmark 3 and uses the ranging device to calculate its distance from these landmarks. The distance measurements are denoted by m11, m12, m13 taken for Landmark 1, 2, 3 respectively. Now at instant I2, the robot moves a certain distance and estimates its states as ($x + dx$, $y + dy$, $\theta + d\theta$) using the dead reckoning technique. Based on the knowledge of its current state, the

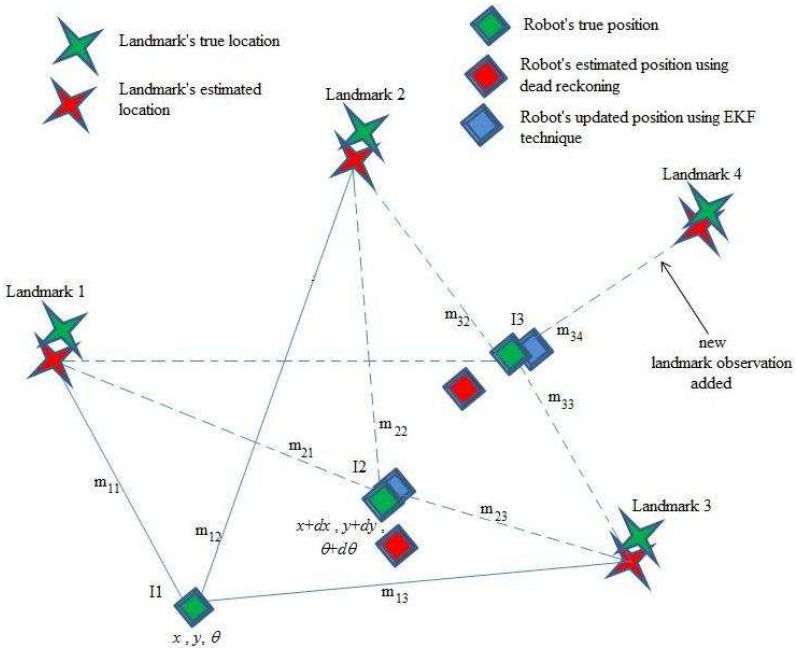

Figure 13: The logic for SLAM algorithm.

robot estimates the position of previously observed landmarks. At the same time the robot obtains range measurements for the previously observed landmark. But, as the robot observes that there is a discrepancy in the estimated landmark position and the observed landmark position (calculated by ranging device), the robot updates its states using the information gained by the ranging devices measurements. It should be noted that the ranging device measurement is trusted more than the dead reckoning technique, because the ranging device has more accuracy as compared to dead reckoning technique. Also, as the ranging measurements are not perfect, accurate localization of the robot cannot be obtained. But the final localization obtained is still closer to the actual position of the robot [22][23]. As shown in figure 13, green color square block represents the true position of the robot, the red color square block represents the robots estimated position using the dead reckoning technique and the

blue color square block represents the updated position of the robot using the EKF technique. Now at instant I3, the robot performs the same procedure, as described for instant I2, to updates its position; only this time it adds new landmark 4 into its measurement list.

Now at instant I2, the part where the robot estimates its state using the dead reckoning technique up to the part where the robot updates its state using the measurements taken by the ranging device defines the EKF technique [22]. Sub-section 2.10 summarizes the steps involved in the Kalman Filtering and the EKF techniques. Most of the part for the Kalman filtering technique has been directly obtained from Bishop, G., Welch, G., An introduction to the Kalman Filter,*Course 8, Presented at ACM SIGGRAPH* (2001).

2.10 Kalman Filter

The Kalman Filtering technique is considered as a solution to discrete-data linear filtering problem and is used particularly in the area of autonomous robot navigation [24].

In order to implement the Kalman Filter technique for a process-

- There should be state defined for a process at a given instance.
- There should be a measuring device (ranging device).
- There should exist a relation between the state and the measurement obtained.

The aim of the Kalman Filtering technique is to use observed (but corrupted with noise) measurements over time and generate values of the state and the measurement that tend to be closer to the true values [24][25].

Therefore, to estimate the state $x \in \Re^n$ of a process defined by the linear stochastic difference equation [24],

$$x_k = Ax_{k-1} + Bu_{k-1} + w_{k-1} \tag{23}$$

by using the knowledge of the measurement $z \in \Re^m$ given by,

$$z_k = H_k x_k + v_k \tag{24}$$

where, x_k is the state vector of the system at k^{th} observation (measurement or iteration),

x_{k-1} is the state vector of the system at $k-1^{th}$ observation (measurement or iteration),

A is the state transition matrix describing the state transition from k^{th} to $k-1^{th}$ observation,

B is the matrix relating control inputs to the state of the system,

u_{k-1} is the control input applied at $k-1^{th}$ observation,

z_k is the k^{th} observation (measurement or iteration),

H is the matrix relating the state (x_k) to the measurement (z_k),

w_{k-1}, v_k represents the process noise and the measurement noise for the given observation, respectively,

with normal probability distribution function given by [24],

$p(w) \approx N(0,Q)$, where Q is the process noise covariance and

$p(v) \approx N(0,R)$, where R is the measurement noise covariance.

The following nomenclature is used in the Kalman Filtering technique,

$\hat{x}_k^-$ represents *a priori* (minus sign in superscript) state estimates (hat) for the observation k (with k at subscript)

$\hat{x}_k$represents*a posteriori* (no sign in superscript) state estimates (hat) for the observation k (with k at subscript)

As stated before the Kalman Filtering technique is use to estimate the state of a system, for which the *a priori* and*a posteriori* estimate errors can be defined as [24],

$$e_k^- \equiv x_k - \hat{x}_k^- \tag{25}$$

$$e_k \equiv x_k - \hat{x}_k \tag{26}$$

Correspondingly, the *a priori* and the *a posteriori* estimate error covariance is defined as,

$$P_k^- = E[e_k^- e_k^{-T}] \tag{27}$$

$$P_k = E[e_k e_k^T] \tag{28}$$

The matrices P_k^- and P_k are important elements in the Kalman Filtering technique as they define the uncertainty in the estimation of the state vector x. A large value of P_k (or P_k^-) indicates that estimated state value $\hat{x}_k$(or $\hat{x}_k^-$) differs the actual state value x by large amount. Similarly, a small value of P_k (or P_k^-) indicates that the estimated state value $\hat{x}_k$(or $\hat{x}_k^-$) differs the actual state value x by small amount. Therefore, along with the state estimation the main objective of the Kalman Filtering technique is to reduce the value of P_k (or P_k^-) to a desired limit, so that the uncertainty between the estimated and the actual state value is reduced [24]. In Kalman Filtering technique, the equation to compute the *a posteriori* state estimate $\hat{x}_k$ is given by the linear combination of the *a priori* state estimation $\hat{x}_k^-$ and the weighted difference between the actual measurement z_k and the measurement prediction $H_k\ x_k$ [24],

$$\hat{x}_k = \hat{x}_k^- + K_k(z_k - H\hat{x}_k^-) \tag{29}$$

The quantity $(z_k - H\hat{x}_k^-)$ in equation(29) is called the measurement *innovation* or the *residual factor* which simply reveals the difference between the predicted measurement $H\hat{x}_k^-$ and the actual measurement z_k [25].

The matrix K_k is defined as the Kalman Filter *gain* or the *blending factor*, which tries to minimize the *a posteriori* state estimation error covariance, and is given by,

$$K_k = P_k^- H^T (H P_k^- H^T + R)^{-1} \tag{30}$$

The idea behind calculating the value of K_k is to assign the *residual factor*, given in equation(29), a value such that the resulting*a posteriori* state vector estimate $\hat{x}_k$ has

a lower error covariance than its *a priori* state estimate value $\hat{x}_k^-$ [25].

The Kalman Filtering technique can be divided into two stages:

- **Estimation stage**: In the estimation stage the values of the *a priori* state and the error covariance matrix are calculated and forwarded to the measurement stage.
- **Measurement/Correction stage**: The (noisy) measurement value is obtained and the values for the state and the error covariance are updated (or corrected) to get *a priori* state and error covariance estimation, using the knowledge of the measurement.

The following flow-chart summarizes the steps involved in the Kalman Filtering technique:

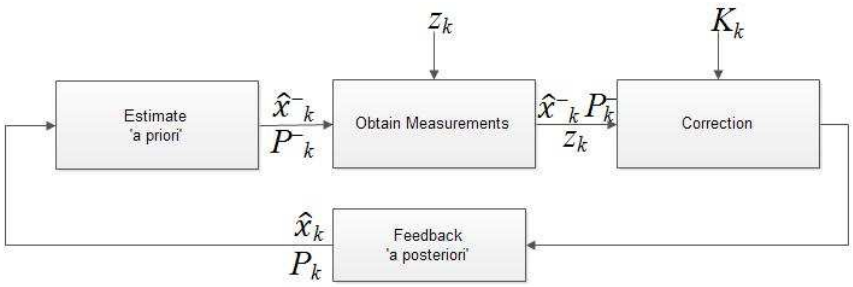

Figure 14: Flow chart for Kalman Filter process.

Figure 14 describes the flow chart for the Kalman filtering process for k^{th} observation. The '*a posteriori*' values for the state and error covariance are estimated using the knowledge of the '*a priori*' values of the state, error covariance and the (calculated) Kalman gain [24] [25]. The flow chart consists of following steps,

- **Estimate 'a priori'**: Estimate the *a priori* values of the state $\hat{x}_k^-$ and the error covariance P_k^- given by the equations,

$$\hat{x}_k^- = A\hat{x}_{k-1} + Bu_{k-1} \tag{31}$$

$$P_k^- = AP_{k-1}^- A^T + Q \tag{32}$$

- **Obtain Measurements**:Obtain measurement z_k for the k^{th} iteration

- **Correction**:Calculate the Kalman filter gain and (update) the *a posteriori* state estimate using the following equations,

$$K_k = P_k^- H^T (HP_k^- H^T + R)^{-1} \tag{33}$$

$$\hat{x}_k = \hat{x}_k^- + K_k(z_k - H\hat{x}_k^-) \tag{34}$$

$$P_k = (I - K_k H)P_k^- \tag{35}$$

- **Feedback 'a posteriori'**: After each iteration, the new estimated *a posteriori* state and the error covariance are calculated and feedback to the initial (estimation) stage as the a priori state and error covariance for new measurement [24][25].

2.11 Extended Kalman Filter

The Extended Kalman Filter (EKF) technique is used in case if the process to be estimated and (or) the measurement relationship to the process is non-linear [24]. The EKF technique is simply the Kalman Filtering technique that linearizes the estimation around the current estimation. In simple words, for the EKF technique the partial derivatives of the process and the measurement functions, governed by some non-linear relationship, are implemented at each iteration[24].

Therefore, given a process with a state vector $x \in \Re^n$ governed by the non-linear stochastic difference equation,

$$x_k = f(x_{k-1}, u_{k-1}, w_{k-1}) \tag{36}$$

with measurement $z \in \Re^m$ given by,

$$z_k = h(x_k, v_k) \tag{37}$$

The function $f(\cdot)$ and $h(\cdot)$, given by equation(36) and (37) respectively, are non-linear functions. The function $f(\cdot)$ relates the state at the previous time step $k-1$ to the state at the current time step k. The function $h(\cdot)$ relates the state x_k to measurement z_k [24].

As the steps involved in EKF technique is similar to that of the Kalman Filtering technique, the state transition matrix A and matrix H in the estimation stage for EKF is given by,

$$A = \frac{\partial}{\partial x} f(\hat{x}_{k-1}, u_{k-1}, 0) \tag{38}$$

$$H = \frac{\partial}{\partial x} h(\hat{x}_{k-1}, 0) \tag{39}$$

Therefore, at each time step the Jacobian matrices (or linearizing matrices) for A and H are calculated and then can be used in the Kalman Filtering technique directly [24].

2.12 Chapter Summary

This chapter introduced various localization systems and the cricket location-aware system. Considering the benefits provided, the cricket system is used in this thesis work for indoor localization. A detail explaination to the localization technique applied by the cricket system is provided. Finally the general theory for the SLAM algorithm and the Kalman Filtering technique is introduced.

3 Experimental Observation

The main objective of this thesis work is to obtain coordinate assignment for the cricket motes autonomously. In order to autonomously assign coordinate points, the cricket motes must have knowledge of the distance measurements from other motes. Hence, it is essential to study the maximum range capacity and accuracy level of the cricket motes.

Section (3.1) introduces to the structure and the working principle of the US transducer. The basic US wave formation is explained in section(3.2). Section(3.3) provides data obatined from various field experiments to understand the behavior of the US sensor of the cricket motes at a particular point.

3.1 Structure and Working of an Ultrasonic Transducer

This section discusses about the structure of the US transducer and the formation of the US pulse in detail. The basic theory for the formation of the US pulse is described by stating few simple examples to get a better understanding.

Figure 15 shows the structure of the piezo-electric transducer used in cricket motes. When an alternating voltage is applied across the piezo-electric material, it starts vibrating. Also, if the piezo-electric material (metal cone) is made to vibrate, charge appears on its surface. Hence, when an alternating voltage of particular amplitude is applied across connectors A and B (Figure 15) the piezo disk starts resonating at a frequency of 40Khz which in-turn causes the metal cone to vibrate. This creates vibrations in the surrounding medium (air), which are nothing but the ultrasonic waves. Thus, for a beacon an alternating voltage is applied across the piezo-electric material to create the US waves; while in case of a listener, the transmitted US waves are detected by sensing the appearance of the charge on the surface of the piezo-electric transducer [19]. Figure 15 also shows three axes (X, Y, Z) for the cricket US

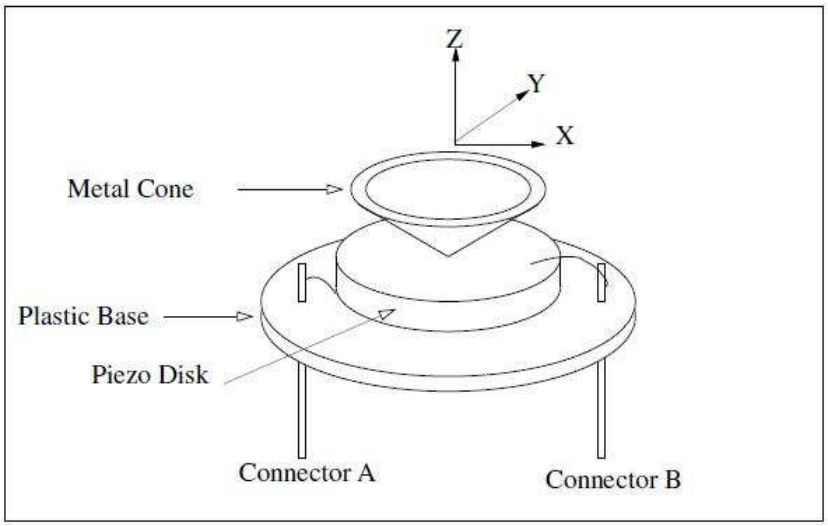

Figure 15: The Piezo electric transducer of cricket mote [19].

transducer. In this project the cricket motes are mounted on a stand, few meters above the ground level in such a way that its Z-axis remains parallel to the ground. For simplicity, the Z-axis of the cricket mote will be directly referred as axis of the cricket mote.

3.2 Behavior of an Ultrasonic wave

This section provides a detail insight to the general behavior of an ultrasonic wave. At instance 1 in figure 16, both the atoms of US transducer surface and that of the air surrounding it are in an equilibrium state.

At instance 2 (figure 17 (a)and(b)) when the voltage is applied to the piezo-electric transducer, atoms of the transducer start vibrating (move back and forth). Thus they collide with the air atoms surrounding the transducer, in-turn making the air atoms to collide with their neighboring atoms or particles. This action leads to transfer of energy from one atom to its adjoining atom or particle, which in-turn leads to oscillatory motions of the atoms or the particle in a given medium (in this case

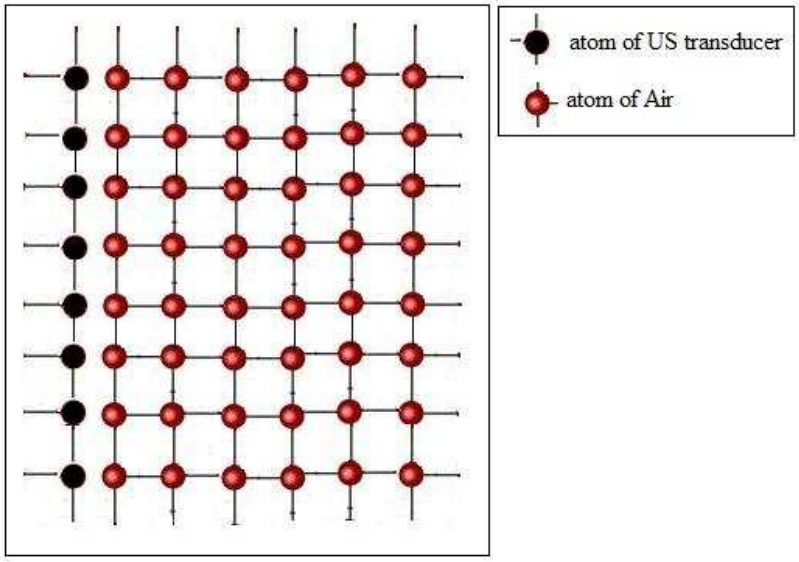

Figure 16: State of the atoms at equilibrium.

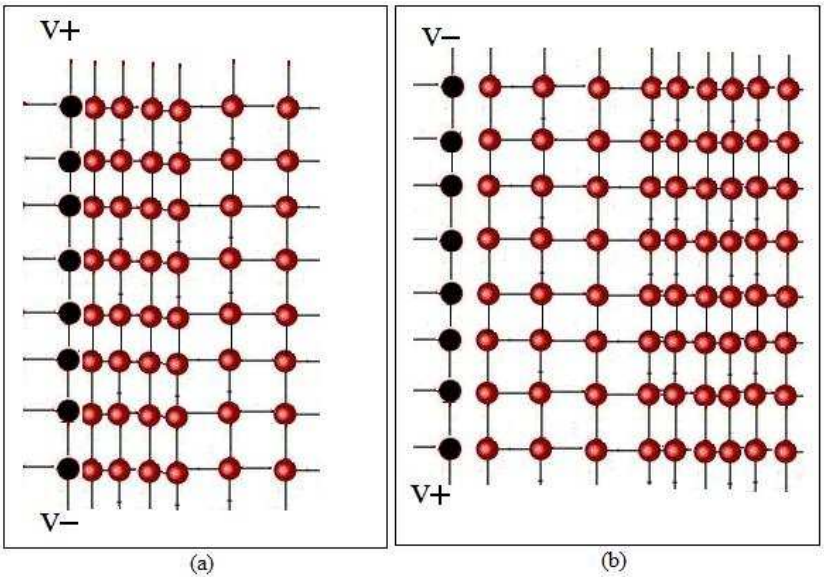

Figure 17: Vibration of the transducer atoms when voltage is applied.

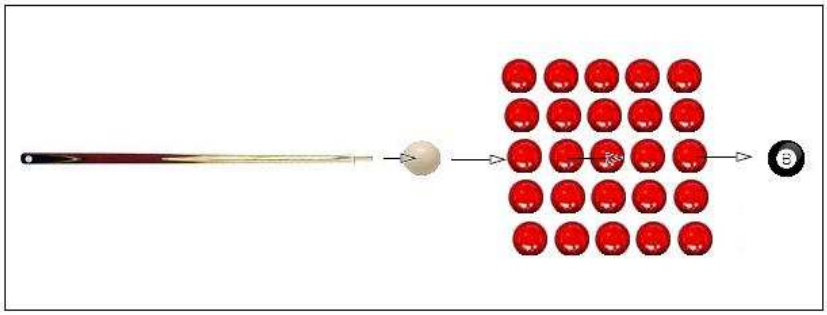

Figure 18: Perfect transfer of energy when balls are arranged in a straight line.

air). In simple terms, US wave can be visualized as an infinite number of oscillating masses or particles connected by means of elastic springs and the oscillation occurs due to transfer of energy from one particle to another. The amplitude of the oscillation of any particle in a given medium is totally dependent on the motion of its nearest neighbor. This phenomenon is observed only when the particles of both (the US transducer and the medium) are perfectly aligned in a straight line [20].

Due to misalignment of the particles, the energy transfer is not always in the direction of the wave propagation, but gets transferred off at an angle. To understand this phenomenon, consider an example for a pool table. Balls are arranged uniformly in the given fashion and are perfectly aligned in a straight line, as shown in figure 17. Now when the cue ball hits the first ball in the center row, energy is transferred from the cue ball to the first ball in the center row. This in-turn causes the cue ball to hit its neighboring one and so-on. The energy transfer is along a straight line and finally the last ball in the center row hits the black ball. It should be noted that the balls in the other rows remains undisturbed.

Figure 18 a situation in which the first ball in the middle row is not arranged in a straight line but rather slightly bit off the center.

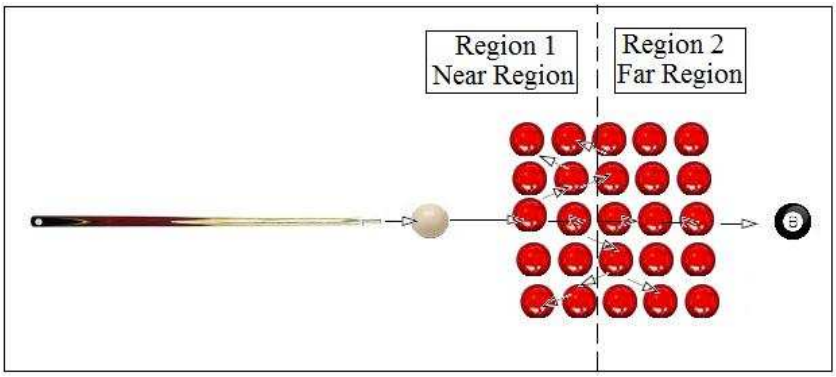

Figure 19: Dispersion of balls when they are not arranged in a uniform straight line.

When the cue ball hits the first ball in the center row (which is slightly off the center line), it does not travel along the straight line. The ball hits other balls in its vicinity and now the entire energy transfer is not along the straight line. Thus, the equilibrium position of balls in all other rows is disturbed and they hit other balls as they try to spread-out. It should be noted that as balls in all rows spread-out, balls lying in Region 1 will spread out to greater extent as compared to balls lying in Region 2. This is because energy transfer is originated in Region 1 by the cue ball. Such, uneven spread of energy (or particle displacement of the medium) is observed in the US wave formation also. Two points to remember from this example are -

1. Even though the energy transfer is uneven, still the energy content along the straight line is always greater because the cue ball was targeted to hit along the straight line.

2. Energy content slowly diminishes for balls away from the center row. Energy content is very low for balls far away from the center line. This can be observed by the amount of displacement from their initial position. Balls in Region 1 (near region) spread out to greater extent as compared to balls in Region 2 (far

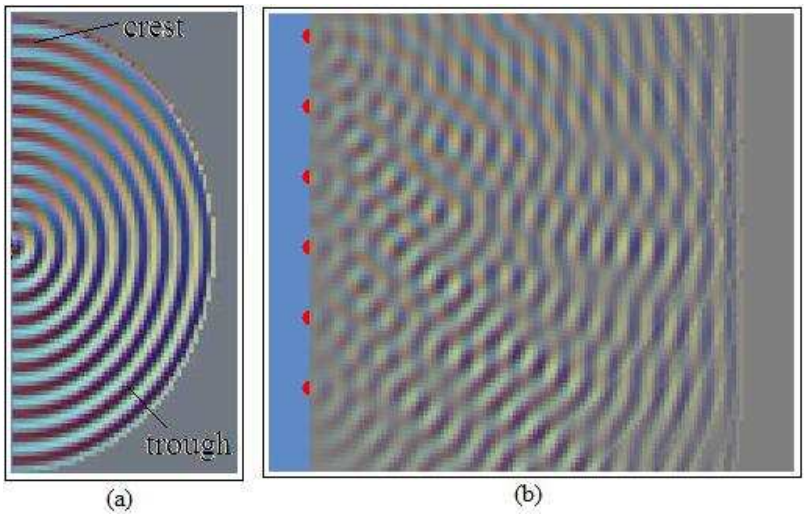

Figure 20: (a) Circular wave front from a single source [20],(b) Circular wave front from multiple sources [20].

region), because of high energy content in Region1. Similarly, in case of US wave, the energy content along the axis of the US transducer is always higher as compared to that for other angles. Energy content in near region of US wave is always greater than that of far region.

From the discussion so far, the formation of the US wave is considered in 2D. Consider the formation of US waves from multiple point sources and in 3D. US waves created by a US transducer travel as a circular wave front [20]. The crest and trough part of the wave front is indicated in figure 20(a). For a given US transducer the US wave originates from multiple points along the surface of the US transducer [21]. This results in formation of multiple US waves simultaneously interacting with each other, as shown in figure 20(b) [20]. To understand the formation of US wave in more simple terms, consider the formation of the waves on a calm water surface. Formation of the US wave from a single point is similar to that of the waves originating from a point on a calm water surface, when a small pebble is dropped at that point. Now

when multiple pebbles are dropped simultaneously at different points, multiple waves are generated which then start interacting with each other as shown in figure 20(b). Similar case is observed in case of an US waves originating from multiple points of a given US transducer, which then interact with each other [20].

In the following three experiments the beacon and the listener are mounted on a stand 1 m above the ground. Mounting both (listener and beacon) 1 m above the ground avoids path loss of the US waves. Path loss is usually caused in ultrasonic wave propagation because of the reflected waves (from shiny surface or floor) interact with the propagating wave. This interaction causes some loss in the overall energy of the wave called as path loss [9]. Thus path loss is avoided by mounting them few meters above the ground. Field experiment has shown that mounting cricket motes 0.5 m above the ground surface yields same results as that for motes mounted at a height of 1 m. But, due to obstacles or shiny reflective floors in an indoor environment, it is advisable to mount the motes at least $1m$ above the ground surface. All the following three experiments are conducted in an indoor air-conditioned environment at 20°C (72° F) and the temperature is assumed to remain constant throughout the experiment.

3.3 Experimental Data

In the following three sections, the behavior of the US sensor of the cricket mote is studied by using the data obtained from the field experiments.

3.3.1 Experiment 1

The purpose for conducting this experiment is to understand the accuracy level in distance measurements obtained at a particular point, when the listener is facing beacon. The graph given in figure 21 is a polar plot for the radiation pattern of the US wave transmitter of the cricket mote (beacon). The beacon is stationed at the

origin of the polar plot facing along the 90° line, as shown in figure 21 and the listener is moved in a circular fashion, but facing the beacon at all instances. The radius of the circles represents the distance separation between the listener and the beacon. The angles (in degrees) represent the angles at which the listener is kept facing the beacon. Initially the listener is kept at a distance of 100 cm (1 m) away from the beacon and at an angle of 0°. The listener is then moved in a circular fashion (along the 1 m radius circle) with an angle increment of 10°. The readings are taken only up till the 180° angle. It is observed that readings are obtained even when the listener is kept behind the beacon for less than 100 cm (1 m). But the region of interest in this project is the region in front of the beacon. Similarly the same procedure is repeated by the incrementing the radius of the circular path by 50 cm (0.5 m). The experiment is conducted until the radius of 1000 cm (10 m) is reached.

The points marked with stars are the points with highest accuracy. These points lie along the 90° line, along which the beacon is facing. The points marked with circles are the points where distance-measurements obtained have error rate up to 4 cm or less. Points marked with cross are the points where the error rate is higher than 4 cm but up to 17 cm. Points between 0° to 180° which are not marked at all, represents the points where distance measurements cannot be obtained even when the listener is facing the beacon. The green block of area 2 m× 8 m is defined as the accuracy zone, created by the beacon. This is a high energy level region and any listener (facing the beacon) inside this area will detect the US wave with less time delay. Hence, the level of accuracy in TDoA measurement will be high. In short the beacon forms a rectangular area of 2 m× 8 m, inside which if the listener is moved facing beacon, then the error obtained in distance measurement is low (less than 4 cm).

The three main points to be concluded from this experiment are -

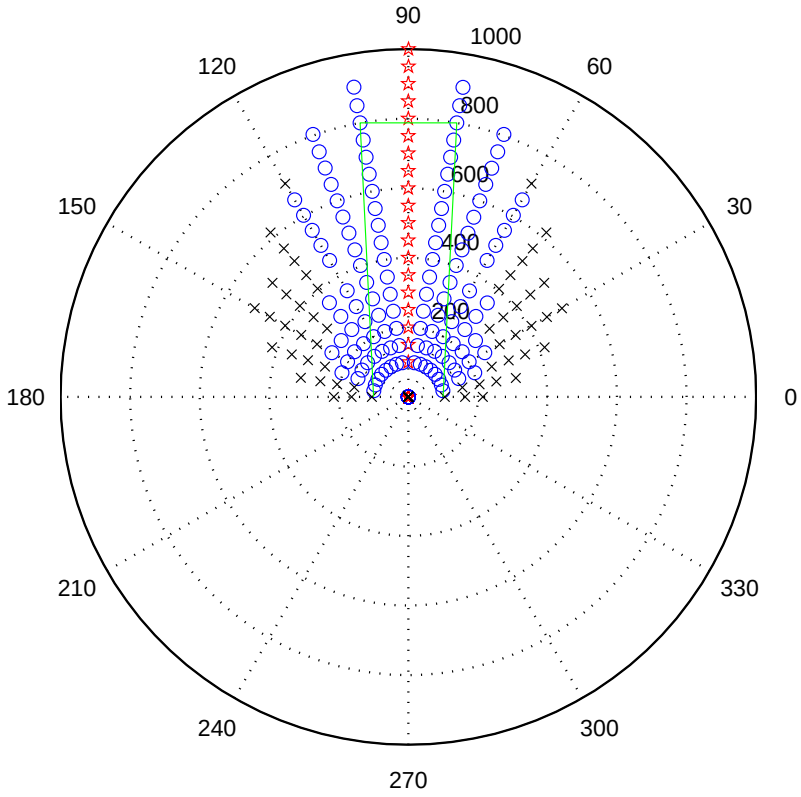

Figure 21: Radiation pattern for the US transducer of the cricket mote.

1. The error along the 90° line is almost zero. Hence the US waves (transmitted by the beacon) have high energy content along the 90°, and they are detected by the listener receiver circuit within no time.

2. As the listener moves away from the 90° line, the energy of the transmitted US wave diminishes slowly. But within an angle of 30°, on both sides of the 90° line (i.e. between angles 60° and 120°), the energy content of the US wave is still high enough for the listener's receiver circuit to detect the US wave. The listener's US wave detector circuit (i.e. two stage programmable amplifier) detects the US wave but with some time-delay. Due to this time delay the

estimated distance value by the cricket mote (listener) is slightly greater than the actual distance value.

3. For points above 120° and below 60° angle, the energy content diminishes to a greater extent, causing the listener's US detector circuit to detect the transmitted US wave with large time-delay. Hence the large time-delay causes the estimated distance value to be greater than the actual distance value resulting in large error in the estimated distance value.

Therefore, when there is an error in the distance estimation, the estimated distance always comes to be greater than the actual distance measurements. It should be noted that, however, this may not always be the case, because the distance estimation is also depended upon the on-board temperature sensor. For a given temperature, the cricket mote calculates the corresponding speed of sound to get the required distance measurement [13].

3.3.2 Experiment 2

Figure 22 shows the field experiment conducted to study the near region of the US wave. In this high fluctuation area, energy content (resultant displacement of the particle) is high enough to cause the receiver circuit of the listener to detect the US wave easily even when the listener is not facing the beacon.

In this experiment beacon is kept stationary at point $(0, 0)$ as shown in figure 22 and axis of the beacon is kept along the Y-axis, i.e. the beacon is facing along Y-axis. Now the listener is initially stationed at point $(1, 0)$. The listener is positioned in such a way that its axis is orthogonal to the axis of the beacon, i.e. listener is facing along the X-axis. Readings are obtained for the distance estimation between the listener and the beacon. Now, the listener is kept at point $(1, 1)$ still facing along the X-axis and readings for the distance estimation are recorded. Thus, the listener's position is

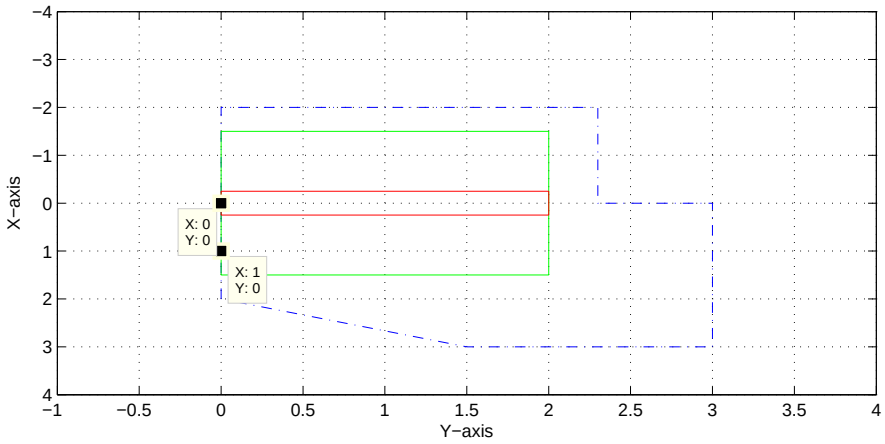

Figure 22: Near region energy content for the cricket mote.

incremented and the distance measurements are recorded. For example, the listener is positioned at $(1, 2)$, $(1, 3)$, $(2, 1)$, $(3, 1)$ and so on until the distance measurements are available. Similarly, the experiment is conducted for the negative X-axis.

The area within the blue border block of the graph shows that the listener is still able to detect the US wave emitted by the beacon, even if the listener is not facing the beacon. The area within red block is the region where no TDoA measurement is obtained. The distance measurements recorded by the listener within the green block but outside the red block shows high level of accuracy (error less than 2 cm). This area is nothing but the accuracy zone for the defined layout of the beacon and the listener. Thus the TDoA measurement obtained by the listener always has high level of accuracy when kept in the accuracy zone. In summary for defined beacon-listener layout, if the listener is kept within an area of 2 m$\times$ 3 m the listener is still able to estimate the distance from the beacon with high level of accuracy.

3.3.3 Experiment 3

In this experiment, intially listener is positioned at point O facing along the line OC (figure 23). Beacon is stationed at a distance of 91 cm from point O, facing along OC and towards point O (figure 23). Therefore the beacon and the listener are facing

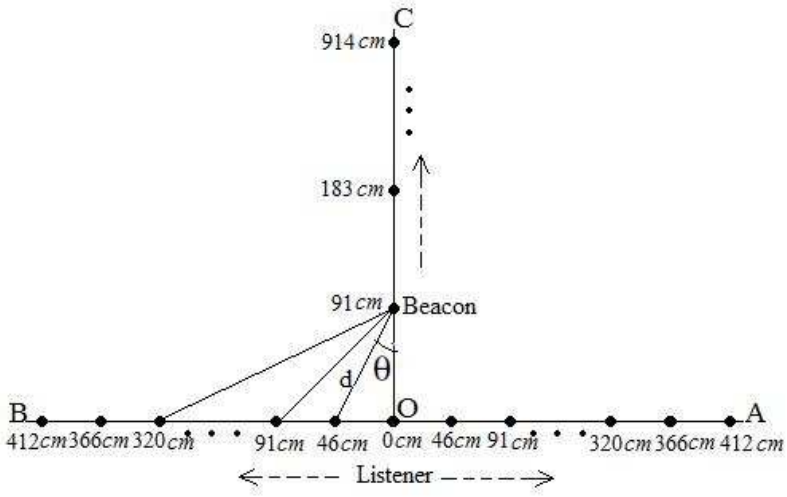

Figure 23: Error in range estimation for a given distance and angle.

each other with their axis lying along line OC. The distance measurement between the beacon and the listener is obtained and the resulting error in the distance measurement is recorded. Now the listener is moved (keeping its axis parallel to line OC) to a point, which is 46 cm away from point O (figure 23). For a given angle θ the distance measurement d is obtained and the resulting error in distance estimation is recorded. The listener is moved along line AB (keeping its axis parallel to line OC), by incrementing its distance from point O in steps of 46 cm. For each point the error resulting in distance estimation and the corresponding angle θ is recorded. The experiment is conducted on both sides of line OC with beacon kept stationary at 91 (from point O). The beacon is stationed at 183 cm, 274 cm, 366 cm,. . ., 914 cm away from point O and the above defined experiment is conducted similarly.

From figure 24 to 28 it is clear that for a given position of the beacon the error in distance estimation d is directly proportional to the value of angle θ, i.e. if the value

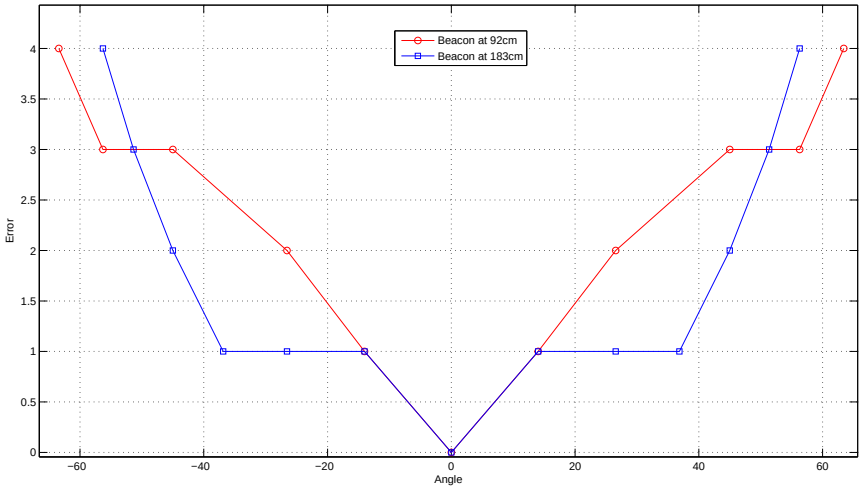

Figure 24: Plot of angle vs. error, for beacon placed at 3FT(92cm) and 6FT(183cm) from point O.

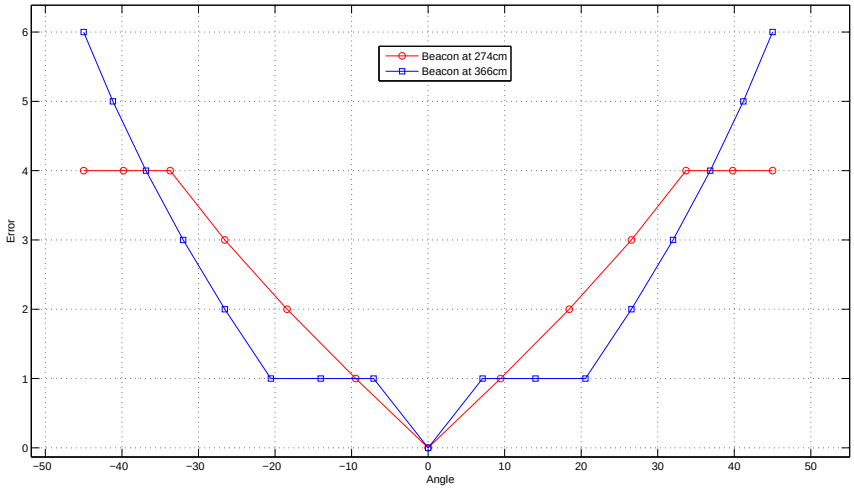

Figure 25: Plot of angle vs. error for Beacon placed at 9FT(274cm) and 12FT(366cm) from point O.

of θ is large the resulting error in the distance estimation by the listener is large and vice versa. Also when beacon is placed from 91cm to 731 cm away from point O, for $-5^\circ \leq \theta \geq 5^\circ$ the error is less than 2 cm, because of the high energy content of the US wave (as explained in section(3.2)). This region is defined as the accuracy zone for

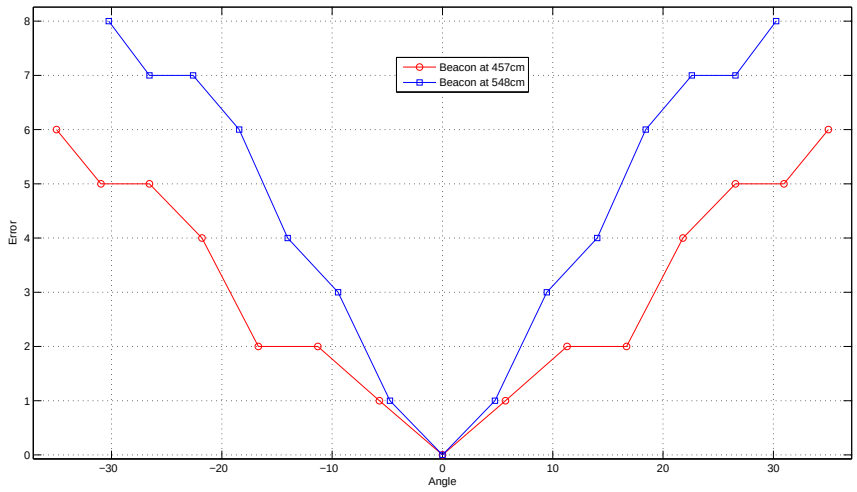

Figure 26: Plot of angle vs. error for Beacon placed at 15FT(457cm) and 18FT(548cm) from point O.

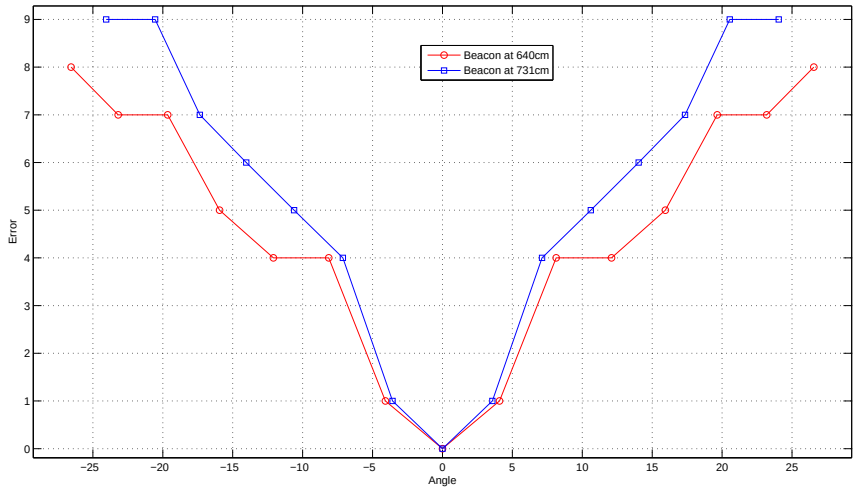

Figure 27: Plot of angle vs. error for Beacon placed at 21FT(640cm) and 24FT(731cm) from point O.

the given beacon-listener layout. Therefore any listener kept within $-5° \leq \theta \geq 5°$ of a beacon, according to the defined beacon-listener layout, has high level of accuracy in distance estimation.

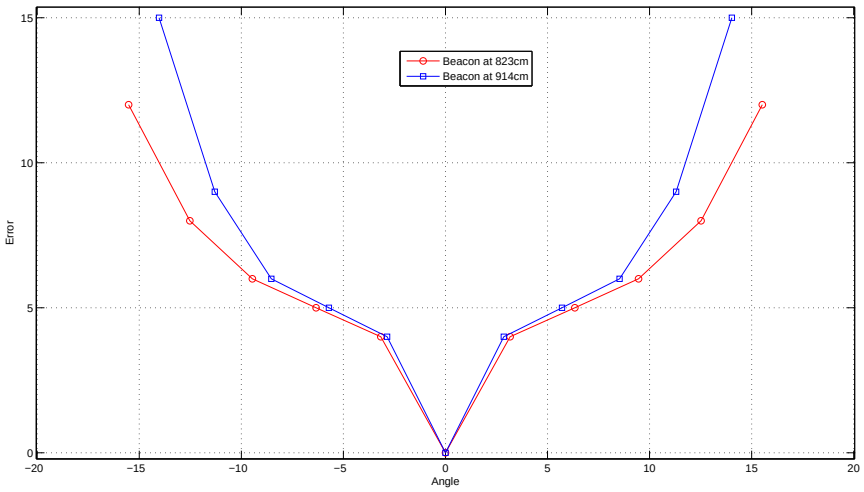

Figure 28: Plot of angle vs. error for Beacon placed at 27FT(823cm) and at 30FT(914cm) from point O.

3.4 Chapter Summary

In summary, this chapter provides a brief detail about the behavior of the US wave and the level of accuracy obtained in distance estimation by the listener for a given beacon-listener layout.

4 Algorithm Formulation

Chapter 3 provided a general detail for the formation of the US waves by an US transducer. The data obtained from the three experiments provide the accuracy level and communication range for the US transducers of the cricket mote. Using this data, the algorithm for the self-calibration of the cricket motes is formulated.

This chapter describes the formulation of the algorithm for the self-calibration of the cricket motes. Section(4.1) describes the procedure for the layout of the cricket motes around a field. The formulation of the algorithm is described in section(4.2). Finally a detail mathematical description for the proposed algorithm is discussed in section(4.3) and (4.4).

In the following discussion the network and the motes are referred using the following nomenclature,

N_i^j:represents the j^{th} mote in i^{th} network, where i = 1,2,3,. . . ,6 and j = 1,2,3 (in this project) with coordinates, (x_i^j, y_i^j). For example, N_2^1 represents the first mote of network 2 with coordinates (x_2^1, y_2^1). Each network, N_i consists of a group of 3 motes (N_i^1, N_i^2, N_i^3).

In order to achieve the self-calibration of the cricket motes, the motes are mounted on a stand 1 m above the ground level. Mounting the cricket motes 1 m above the groung level, allows to obtain the inter-mote distance measurements and avoids path loss. It should be noted that the proposed algorithm focuses on the localization of the cricket motes in 2D space. Hence, the motes are assumed to be maintained in the same plane, i.e in the XY-plane with the z-coordinate equal to zero.

Figure 29 a shows the front view of a network consisting of three cricket motes which are maintained in the same plane. Figure 29 b shows the top view of the network with the green color dots showing the position of the motes N_i^1, N_i^2, N_i^3 fix

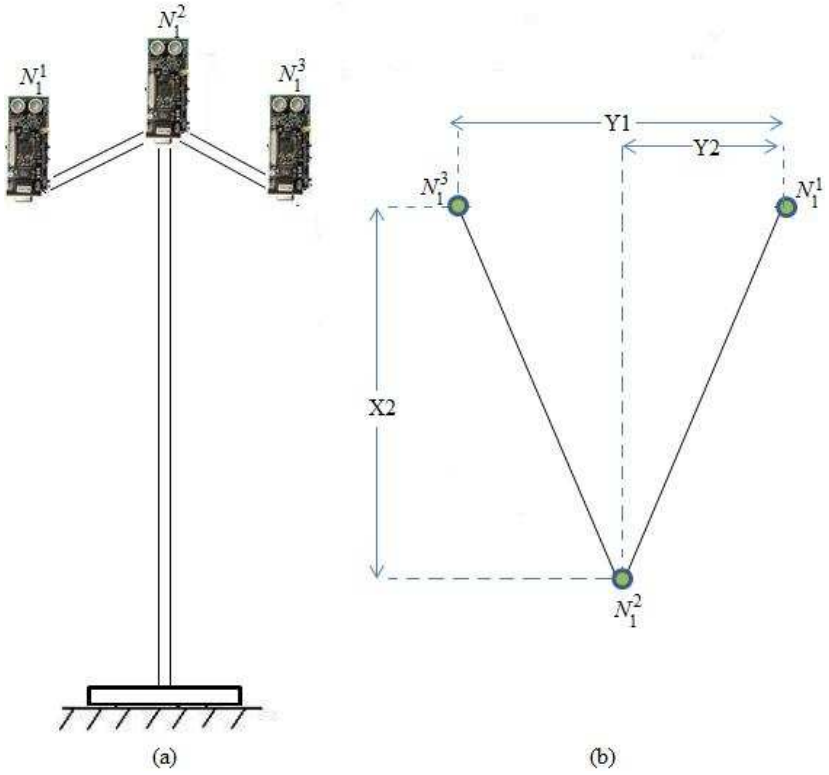

Figure 29: Network with three cricket motes (a)Front view, (b)Top view.

on the stand. The relation between the x and y coordinates of motes N_i^2 and N_i^3 with respect to x and y coordinate N_i^1 is given by,

$$x_i^2 = |x_i^1| + X2 \tag{40}$$

$$y_i^2 = |y_i^1| - Y1 \tag{41}$$

$$x_i^3 = |x_i^1| \tag{42}$$

$$y_i^3 = |y_i^1| - Y2 \tag{43}$$

where, $Y1 = 2 \times Y2$ and the values of the variables $X1$, $X2$, $Y1$ and $Y2$ are known to every mote and these values are maintained same for every network. Therefore if the mote N_1^1 is able to obtain its coordinates, then by using the relationship given by

equations(40) to (43), the coordinates for motes N_1^2 and N_1^3 can be obtained.
Equations (40) to (43) describe a way of finding the magnitudes (absolute values) for x and y coordinates of motes N_i^2, N_i^3 if the x and y coordinate of mote N_i^1 is known. Therefore the coordinate values for motes N_i^2, N_i^3 is given by,

$$\text{If,} \mathrm{x}_i^1 > 0$$
$$\mathrm{x}_i^2 = +x_i^2$$
$$\mathrm{x}_i^3 = +x_i^3$$
$$\text{else,}$$
$$\mathrm{x}_i^2 = -x_i^2$$
$$\mathrm{x}_i^3 = -x_i^3$$

The y-coordinate of each network is always positive as per the layout procedure followed,

$$\mathrm{y}_i^2 = +y_i^2$$
$$\text{and } \mathrm{y}_i^3 = +y_i^3$$

4.1 Layout Technique

This section presents the general procedure followed for the layout of the cricket motes, in order to achieve the localization of the cricket motes autonomously. It should be noted that the length of the field to be mapped should be an even number.

Figure 30 shows a floor plan for a manufacturing plant, and the area to map is shown in shaded region (between the finished goods and conveyer belt). The given plan is for an indoor location where no GPS signals can be received. Consider an autonomous robot (autonomous fork-lift) which needs its pin-point location at every instance in order to transport the finished goods from storage area to the service area and also to avoid obstacles at a known locations.

For a given field of area L m$\times$ 5 m ($length \times breadth$), the total number of motes (T)

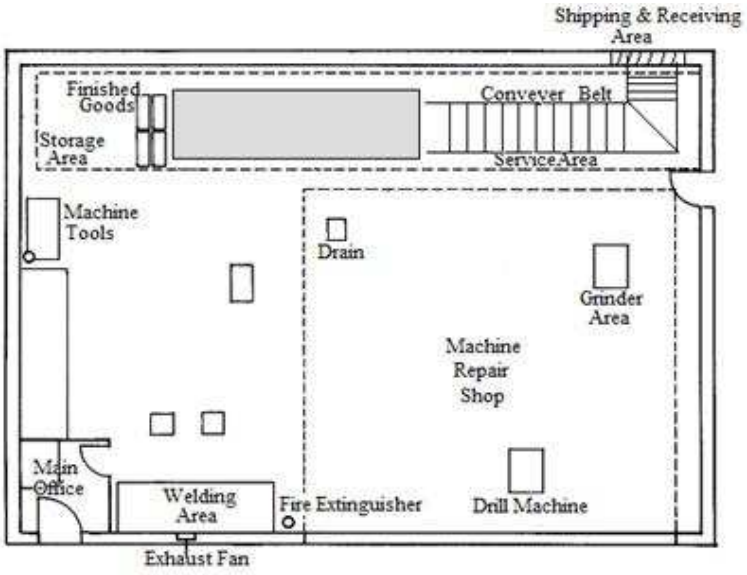

Figure 30: Floor Plan for a Manufacturing Factory.

required to map are given by,

$$T = (L \times 3) + 2motes \tag{44}$$

where, L is an even number and the length of the field.

Assume that the shaded region to be mapped has an area of 6 m$\times$ 5 m. Therefore, the total number of motes (T) required is given by,

$$T = (6 \times 3) + 2 = 20motes \tag{45}$$

These 20 motes cricket motes are then placed around the field to achieve the mapping for the given location as shown in figure 31.

The steps followed in the cricket mote layout are -

1. Motes A and B are placed facing each other on the field border at a distance d_1.

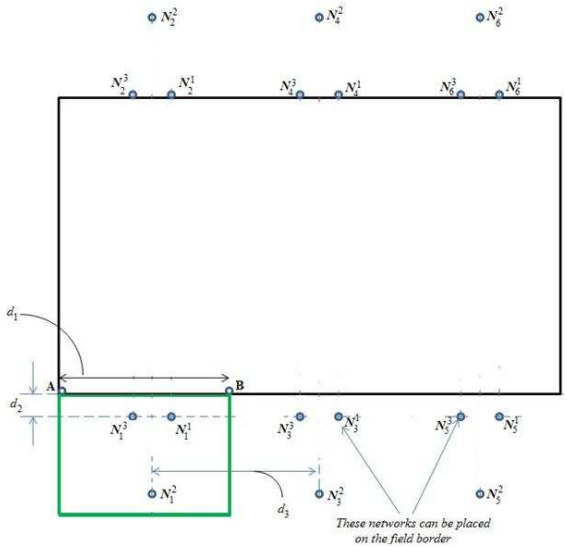

Figure 31: The layout of the cricket motes around a field.

2. Motes N_1^1 and N_1^3 of network N_1 are kept at a distance of d_2 from the field border.

3. Network N_2 is kept facing network N_1.

4. The adjacent networks N_i and N_j are placed such that the mote N_i^2 of network N_i is at a distance of d_3 from mote N_j^2 of network N_j where $i \neq j$ and $i, j = 1$, 2, 3, 4, 5, 6.

1. **Layout of motes A and B**: Motes A and B are placed on the border of the rectangular field facing each other at a distance $d_1 = 2$ m. Therefore, the accuracy in calculating the distance measurement is high (Experiment 1 discussed in section (3.3.1)).

   Now motes A and B form a high energy area of 2 m$\times$ 1.5 m shown by a rectangular box in figure 31 (Experiment 2 discussed in section (3.3.2)). Therefore, any cricket mote (listener) placed in this area is able to obtain the distance mea-

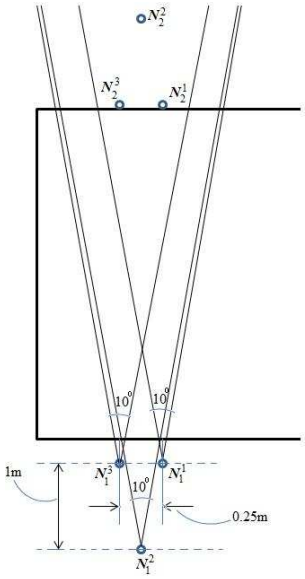

Figure 32: Accuracy zone for the three cricket motes of network N_1.

surements from A and B with high accuracy. Therefore, the motes in network N_1 are placed within this area.

2. **Layout for motes N_1^1, N_1^2 and N_1^3**: Motes N_1^1 and N_1^2 of network N_1 are placed at a distance of d_2 equal to 0.25 m from the field border. This is because the accuracy obtained in TDoA measurement by a listener is high at such a distance (Experiment 2 discussed in section (3.3.2)).

3. **Layout for motes N_1^2**:Network N_2 is kept facing network N_1. The length Y_1 defined in equation(41) is equal to 0.25m.

   Figure 32 shows the reason why the length $Y1$ should be kept equal to 0.25 m. By keeping the motes N_1^1 and N_1^3 0.25 m apart, motes N_2^1, N_2^2 and N_2^3 of network N_2 fall within the accuracy zone of motes N_1^1, N_1^2 and N_1^3. Hence the distance measurements obtain by motes (listeners) N_2^1, N_2^2 and N_2^3 from motes (beacons) N_1^1, N_1^2 and N_1^3 have high accuracy.

The length $X2$ given by equation(40) is equal to 1 m, to achieve good geometric layout. It is also the maximum value for $X2$, because if the value of $X2$ is increased beyond 1 m, then the accuracy obtained in distance measurement by motes N_2^3 and N_2^1 from mote N_1^2 is very low (Experiment 3 discussed in section (3.3.3)).

4. **Distance between adjacent networks**: Experimental results (Experiment1) have shown that the beacon can provide good localization service for a listener with in an area of 2 m$\times$ 8 m. Therefore, every network can cover an area of 2m$\times$ 8 m. Hence, the adjacent networks N_i and N_j are placed such that, the mote N_i^2 of network N_i is at a distance of d_3 from mote N_j^2 of network N_j.
   For a field of area 2 m$\times$ 5 m, a single network is sufficient to cover the whole area to provide the localization service. But using two networks for the same field provides good localization, as they both represent good geometry.

4.2 Algorithm Formulation

The following flow-chart summarizes the steps observed in the self-mapping of cricket motes for 2D localization.

The proposed algorithm is implemented in two phases. In phase 1, the trilateration method is implemented to get rough estimates of the coordinates (states) of each mote. In phase 2, the EKF technique is implemented so as to get a good estimate of the motes compared to that obtained using the trilateration technique in phase 1. In phase 1 -

- **ON**: Switch ON all motes.
- **A in TX All in RX**: The anchor mote 'A' in beacon mode transmits (TX) its US and RF signal while all other motes in listener mode receive (RX) these signals.

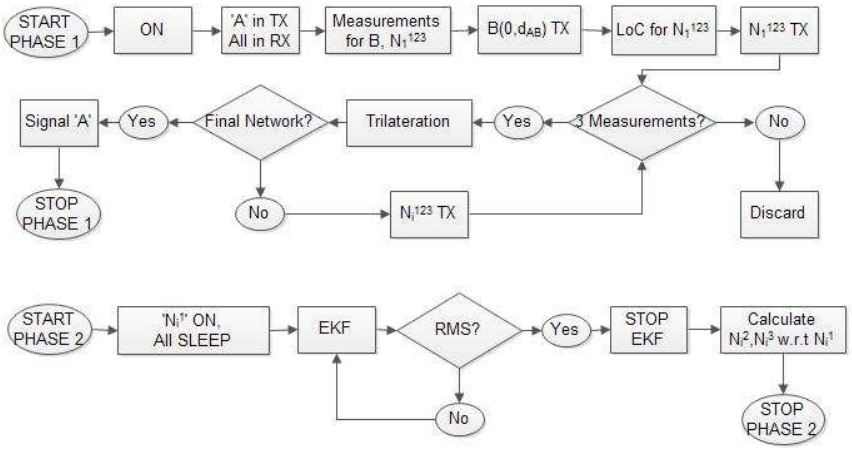

Figure 33: Flow chart for the self-calibration of the cricket motes.

- **Measurements for B,** N_1^{123}: According to the experimental data (experiment 2) only motes B, N_1^1 N_1^2 N_1^3 receive the US and RF pulse transmitted by mote A and calculate their distance from A using the TDoA technique.

- **B(0,d_{AB})TX**:Mote B, the second anchor node, configures its coordinate as (0,d_{AB}) i.e. the Y-axis of the coordinate system passes through mote B. d_{AB} is the distance between A and B calculated using the TDoA technique. B transmits its US and RF signals.

- **LoC for** N_1^{123}: The three motes in network N_1 calculate their coordinates using 'Law-of-Cosines'.

- N_1^{123} **TX**: The three motes in network N_1 now transmit their US and RF signal.

- **3 Measurements**: If three measurements (three coordinates and distances) are obtained from the required network, then coordinates are calculated using the method of trilateration.

- **Final Network**: If all the given networks are mapped, then signal anchor mote

A to start phase 2 or else continue with the mapping.

In phase 2-

- N_i^1 **ON, All SLEEP**: Mote N_i^1 of each network remains in ON state, while rest of the motes goes to sleep mode.
- **EKF**: The EKF technique is implemented using state and distance information between a pair of motes.
- **RMS?**: Check if the desired root mean square (RMS) localization error value is achieved.
- **Calculate** N_i^2**,** N_i^3 **w.r.t** N_i^1:Calculate the coordinates for motes N_i^2, N_i^3 with respect to the calculated values of N_i^1 and stop phase 2.

It should be noted that the EKF technique is applied because the relation between the states (coordinates) and the measurements (given by Euclidean distance formula) is non-linear.

4.3 Mathematical Formulation for Phase 1

This section describes the step-by-step mathematical formulation for phase 1. The following nomenclature is used to represent the distance between two motes for two different networks:

$d_{N_i^j N_i^j}$ represents the distance measurements obtained between mote N_i^j of network N_i and mote N_i^j of network N_i using the TDoA technique. For example, $d_{N_2^1 N_1^1}$ represents the distance measurement obtained between mote N_2^1 of network N_2 and mote N_1^1 of network N_1 using the TDoA technique; with mote N_2^1 as the listener and mote N_1^1 as the beacon, i.e. the TDoA measurement is calculated at mote N_2^1.

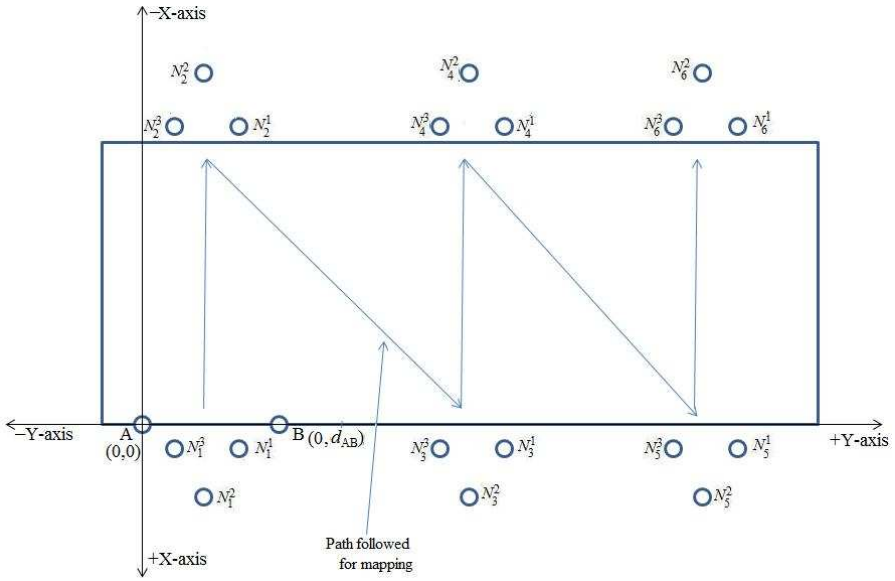

Figure 34: Localization of the motes in phase 1.

Figure 34 shows the top view of the field and the layout of the cricket motes. The path followed for the localization of the networks for mapping of the motes is in zigzag fashion.

1. In Phase 1, all motes are in listener mode except for mote A which is in beacon mode. Mote A $(0, 0)$ transmits its US and RF signals and motes B, N_1^1, N_1^2, N_1^3 calculate their distance from mote A using the TDoA technique. The RF signal of mote A contains the mote ID (A in this case) and its coordinates $(0, 0)$.

2. Assuming that mote B lies at a distance of d_{AB}. B configures its coordinates as $(0, d_{AB})$. Therefore B lies on the Y-axis or in other words Y-axis passes through the point B (Figure 31). As mote B has configured its coordinates, it changes to beacon mode and transmits its US and RF signal. Only motes N_1^1, N_1^2, N_1^3 are able to calculate the distance from mote B using the TDoA technique. The RF signal of mote B contains the mote ID (B in this case) and its coordinates $(0, d_{AB})$.

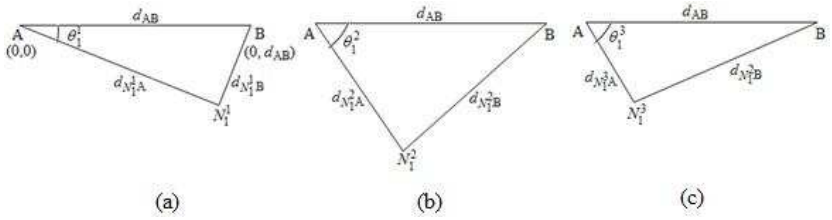

Figure 35: Localization of motes N_1^1, N_1^2, N_1^3 using the law-of-cosines.

3. Now motes N_1^1, N_1^2, N_1^3 know their distance from mote A and mote B and also know the distance between mote A and mote B, i.e. d_{AB}. Therefore, N_1^1 configures its coordinates as,

   Figure 35 shows the procedure for localization of the motes N_1^1, N_1^2, N_1^3 using the law-of-cosines. The angles θ_1^1,θ_1^2 and θ_1^3 are subtended by motes N_1^1, N_1^2, N_1^3 respectively at the origin.

$$\theta_1^1 = \arccos\left(\frac{d_{N_1^1A}^2 + d_{AB}^2 - d_{N_1^1B}^2}{2 \cdot d_{N_1^1A} \cdot d_{AB}}\right) \tag{46}$$

$$x_1^1 = d_{N_1^1A} \cdot \sin\theta_1^1 \tag{47}$$

$$y_1^1 = d_{N_1^1A} \cdot \cos\theta_1^1 \tag{48}$$

   Mote N_1^2 configures its coordinates as (figure 32),

$$\theta_1^2 = \arccos\left(\frac{d_{N_1^2A}^2 + d_{AB}^2 - d_{N_1^2B}^2}{2 \cdot d_{N_1^2A} \cdot d_{AB}}\right) \tag{49}$$

$$x_1^2 = d_{N_1^2A} \cdot \sin\theta_1^2 \tag{50}$$

$$y_1^2 = d_{N_1^2A} \cdot \cos\theta_1^2 \tag{51}$$

   and mote N_1^3 as (figure 32),

$$\theta_1^3 = \arccos\left(\frac{d_{N_1^3A}^2 + d_{AB}^2 - d_{N_1^3B}^2}{2 \cdot d_{N_1^3A} \cdot d_{AB}}\right) \tag{52}$$

$$x_1^3 = d_{N_1^3 A} \cdot \sin\theta_1^3 \tag{53}$$

$$y_1^3 = d_{N_1^3 A} \cdot \cos\theta_1^3 \tag{54}$$

Therefore, motes $N_1^1(x_1^1,\ y_1^1)$, $N_1^2(x_1^2,\ y_1^2)$ and $N_1^3(x_1^3,\ y_1^3)$ are localized using law-of-cosines.

4. After all the motes in network N_1 are localized, they now switch to beacon mode. Beacon N_1^1 transmits it's US and RF signal. The RF signal of mote N_1^1 contains the mote ID (N_1^1 in this case) and its coordinates $(x_1^1,\ y_1^1)$. Motes of network N_2 are preprogrammed to receive the RF and US signals transmitted by the motes of network N_1. Therefore motes $N_2^1,\ N_2^2,\ N_2^3$ receive the node ID via RF signal and calculate their distance from mote N_1^1 using the TDoA technique.

5. After mote N_1^1 has transmitted (US and RF signal), mote N_1^2 transmits followed by mote N_1^3.

6. Motes $N_2^1,\ N_2^2,\ N_2^3$ receive three measurements (three coordinates and three distance measurements) from network N_1 and calculate their own position using the trilateration technique. For example, mote N_2^1 receives three coordinates $(x_1^1,\ y_1^1)$, $(x_1^2,\ y_1^2)$, $(x_1^3,\ y_1^3)$ and three distance measurements $d_{N_2^1 N_1^1}$, $d_{N_2^1 N_1^2}$ and $d_{N_2^1 N_1^3}$ from network N_1 and calculate its location by solving the following equations simultaneously,

$$(x_2^1 - x_1^1)^2 + (y_2^1 - y_1^1)^2 = d_{N_2^1 N_1^1}^2 \tag{55}$$

$$(x_2^1 - x_1^2)^2 + (y_2^1 - y_1^2)^2 = d_{N_2^1 N_1^2}^2 \tag{56}$$

$$(x_2^1 - x_1^3)^2 + (y_2^1 - y_1^3)^2 = d_{N_2^1 N_1^3}^2 \tag{57}$$

where, variables x_2^1 and y_2^1 are the x and y coordinates of the mote N_2^1.

Similarly, motes N_2^2 and N_2^3 localizes themself using the trilateration technique.

Therefore, all the motes in network N_2 are localized and will change to beacon mode.

7. Now, mote N_2^1 of network N_2 transmits its US and RF signal followed by mote N_2^2 and N_2^3. Motes of network N_3 are pre-programmed to receive the three measurements from network N_2 only. So the motes of network N_3 localize themselves using the trilateration technique. Therefore network N_2 assists network N_3 in localization.

8. Network N_3 assists network N_4 in localization as network N_4 is pre-programmed to receive measurements from network N_3.

9. Network N_4 assists in localization of network N_5 and later network N_5 assists in localization of network N_6. Therefore, the localization of each network follows a zigzag path from network N_1 to N_6

Phase 1 allows each mote to get a rough estimate of its location. But due to error in distance measurements calculation, the localization of the motes is not accurate and may contain large amount of error.

It should be noted that in Phase 1, the mapping of network N_1 has high accuracy and can be trusted (experiment 2). As network N_2 is facing network N_1, the amount of error is less in mapping the motes of network N_2 (experiment 3).

4.4 Mathematical Formulation for Phase 2

Phase 1 provides a rough estimate for the location of each motes. After the completion of phase 1, all the motes go to sleep mode, except for mote N_i^1 of each network (i = 1, 2, ..., 6). In this phase, the EKF (Extended Kalman Filter) technique is applied to correct the estimated position of motes N_i^1 obtained in phase 1. The equations for

EKF technique are given by,

$$\hat{x}_k^- = A\hat{x}_{k-1} + Bu_{k-1} \tag{58}$$

$$P_k^- = AP_{k-1}^- A^T + Q \tag{59}$$

$$K_k = P_k^- H^T (HP_k^- H^T + R)^{-1} \tag{60}$$

$$\hat{x}_k = \hat{x}_k^- + K_k(z_k - H\hat{x}_k^-) \tag{61}$$

$$P_k = (I - K_k H)P_k^- \tag{62}$$

It should be noted that all the variables defined in equations (58) to (62) are expressed in the matrix form.

4.4.1 The state estimation matrix $\hat{x}_k^-$

For SLAM algorithm, the state estimation matrix $\hat{x}_k^-$ typically contains the estimate of position and orientation of the robot (x, y, θ) and the position of each landmark (x_l, y_l) [23]. In this project, since no robot is used and the motes are stationary, the matrix $\hat{x}_k^-$ simply represents the position of the motes. Initially the state estimation matrix $\hat{x}_k^-$ contains the value for the position of the mote N_i^1 for each network N_i obtained using the method of trilateration. Therefore, the initial value of the state estimate $\hat{x}_k^-$ is given by,

$$\hat{x}_0 = \begin{bmatrix} \hat{x}_1^1 & \hat{y}_1^1 & \hat{x}_2^1 & \hat{y}_2^1 & \hat{x}_3^1 & \hat{y}_3^1 & \hat{x}_4^1 & \hat{y}_4^1 & \hat{x}_5^1 & \hat{y}_5^1 & \hat{x}_6^1 & \hat{y}_6^1 \end{bmatrix} \tag{63}$$

The hat on each variable represents the estimated values of the motes position.

4.4.2 The matrix A

The matrix A defined in equation (58) represents the state transition matrix. The matrix A is the Jacobian matrix for the prediction model of the robot. Prediction model computes the expected position of the robot, given the previous position and

the cotrol inputs of the robot. Prediction model is usually a function of the position and orientation (x, y, θ) of the robot [23]. For example, for the prediction model,

$$M = \begin{bmatrix} f_1(x,y,\theta) \\ f_2(x,y,\theta) \\ f_3(x,y,\theta) \end{bmatrix} \tag{64}$$

The matrix A is defined as

$$A = \begin{bmatrix} \frac{\partial}{\partial x} f_1(x,y,\theta) & \frac{\partial}{\partial y} f_1(x,y,\theta) & \frac{\partial}{\partial \theta} f_1(x,y,\theta) \\ \frac{\partial}{\partial x} f_2(x,y,\theta) & \frac{\partial}{\partial y} f_2(x,y,\theta) & \frac{\partial}{\partial \theta} f_2(x,y,\theta) \\ \frac{\partial}{\partial x} f_3(x,y,\theta) & \frac{\partial}{\partial y} f_3(x,y,\theta) & \frac{\partial}{\partial \theta} f_3(x,y,\theta) \end{bmatrix} \tag{65}$$

In this thesis, the motes are used instead of robot for localization of a particular location. Also the motes are stationary and contain no dynamics. Therefore, the state transition matrix A is represented by,

$$A = \begin{bmatrix} \frac{\partial}{\partial x_1} x_1 & \frac{\partial}{\partial y_1} x_1 & \frac{\partial}{\partial x_2} x_1 & \frac{\partial}{\partial y_2} x_1 & \cdots & \frac{\partial}{\partial x_6} x_1 & \frac{\partial}{\partial y_6} x_1 \\ \frac{\partial}{\partial x_1} y_1 & \frac{\partial}{\partial y_1} y_1 & \frac{\partial}{\partial x_2} y_1 & \frac{\partial}{\partial y_2} y_1 & \cdots & \frac{\partial}{\partial x_6} y_1 & \frac{\partial}{\partial y_6} y_1 \\ \vdots & & & & \ddots & & \vdots \\ \frac{\partial}{\partial x_1} y_6 & & & \cdots & & & \frac{\partial}{\partial y_6} y_6 \end{bmatrix} \tag{66}$$

$$A = \begin{bmatrix} 1 & 0 & 0 & 0 & \cdots & 0 & 0 \\ 0 & 1 & 0 & 0 & \cdots & 0 & 0 \\ \vdots & & & & \ddots & & \vdots \\ 0 & & & \cdots & & & 1 \end{bmatrix} = I \tag{67}$$

where I is the 12×12 identity matrix.

4.4.3 The Matrix B

Matrix B relates the control inputs u_k to the states of the system [23]. Since no robot is used and the motes are stationary, hence no control inputs are applied, and therefore $Bu_{k-1} = O_{n\times 1}$. Therefore, equation(58) can be written as,

$$\hat{x}_k^- = I\hat{x}_{k-1} + O = \hat{x}_{k-1} \tag{68}$$

4.4.4 The Matrix P

In the Kalman filtering technique, the matrix P is the error covariance matrix for the state estimation. The diagonal elements for the matrix P represents the variance for the state estimated value, i.e. the measure by which the estimated state value ($\hat{x}_i$) differs from its actual value (x_i). The off-diagonal elements for matrix P represents the covariance for the state estimation for two different networks [22][23].

$$P = \begin{bmatrix} \sigma_{x_1}^2 & \sigma_{x_1 y_1} & \cdots & \sigma_{x_1 y_6} \\ \sigma_{y_1 x_1} & \sigma_{y_1}^2 & \cdots & \sigma_{y_1 y_6} \\ \vdots & \vdots & \ddots & \vdots \\ \sigma_{y_6 x_1} & \sigma_{y_6 y_1} & \cdots & \sigma_{y_6}^2 \end{bmatrix} \tag{69}$$

According to discussion in section (4.1) the error in the state estimation (position estimation) for mote N_1^1 is almost zero; hence the estimated values for x_1 and y_1 can be trusted. Therefore,

$$\sigma_{x_1}^2 = \sigma_{y_1}^2 = 0 \tag{70}$$

In case of estimation of position for mote N_2^1, the mapping is also almost accurate (according to discussion in section (4.1)). As both state values contains small amount of error, the value for $\sigma_{x_2}^2$and $\sigma_{y_2}^2$ should contain some non-zero value. But for a 2D coordinate system, there are 3 degrees of freedom. So it is essential that three state values should be fixed or should be trusted so as to have a robust coordinate system. If estimated positions of at least three points are not trusted, then the coordinate system formed by the cricket motes may rotate in wrong direction and the final mapping may have large errors.

So, any one coordinate of the mote N_2^1 should be trusted, even if they contain small

error. Hence, x coordinate of mote N_2^1 is trusted,

$$\sigma_{x_2}^2 = 0 \tag{71}$$

and y coordinate of mote N_2^1 has error in localization for which,

$$\sigma_{y_2}^2 = 99 \tag{72}$$

The value for $\sigma_{y_2}^2$ can be initialized by any non-zero value. In this thesis work the value is chosen as 99.

As the error in localization increases for motes of network N_3 to network N_6 the value of the diagonal elements $\sigma_{x_3}^2$,..., $\sigma_{y_6}^2$ is initialized as,

$$\sigma_{x_3}^2 = \sigma_{y_3}^2 = \cdots = \sigma_{x_6}^2 = \sigma_{y_6}^2 = 99 \tag{73}$$

The values of the non-diagonals elements are initialized to a zero value. This is mainly because the error in the position estimation of each mote is known, but the amount of correlation between the errors in estimating the position of two different motes are not known. Therefore the error covariance matrix P is given by,

$$P = \begin{bmatrix} 0 & & & & \cdots & & 0 \\ \cdot & 0 & & & \cdots & & 0 \\ \cdot & & 0 & 0 & \cdots & & 0 \\ & & & 99 & & & \cdot \\ & & & & 99 & & \vdots \\ \vdots & & & & & \ddots & 0 \\ 0 & & & & \cdots & 0 & 99 \end{bmatrix} \tag{74}$$

The value of diagonal elements of the matrix P gives the amount of uncertainty in the estimated value of each motes. So the main objective is to decrease the value of each diagonal element in the error covariance matrix P, so that the estimated state values (almost) equals its true value.

4.4.5 The matrix H

The matrix H is the Jacobian matrix for the measurement model. The measurement model defines the method by which the range measurement is carried out [23]. In this project, the range measurement or the distance between the beacon and the listener is calculated using the TDoA technique. The distance measurements calculated using the TDoA technique can be represented in terms of its states by using the Euclidean distance formula.

For example, if the TDoA measurement is taken between mote N_q^1 (listener) of network N_q and mote N_p^1 (beacon) of network N_p , then the measurement model can be defined as,

$$z_{N_q^1 N_p^1} = \sqrt{(\hat{x}_q^1 - \hat{x}_p^1)^2 + (\hat{y}_q^1 - \hat{y}_p^1)^2} \tag{75}$$

Where variables $\hat{x}_q^1$ and $\hat{y}_q^1$ represents the estimated states for mote N_q^1 and $\hat{x}_p^1$, $\hat{y}_p^1$ represents the estimated states for mote N_p^1. For simplicity the variable $z_{N_q^1 N_p^1}$ will be represented as $z_{q,p}$.

$$z_{q,p} = z_{N_q^1 N_p^1} = \sqrt{(\hat{x}_q^1 - \hat{x}_p^1)^2 + (\hat{y}_q^1 - \hat{y}_p^1)^2} \tag{76}$$

Then the matrix H for TDoA measurement taken between mote N_q^1 (listener) of network N_q and mote N_p^1 (beacon) of network N_p is defined as,

$$H_{q,p} = \left[\begin{array}{cccccccccccc} \frac{\partial z_{q,p}}{\partial \hat{x}_1^1} & \frac{\partial z_{q,p}}{\partial \hat{y}_1^1} & \frac{\partial z_{q,p}}{\partial \hat{x}_2^1} & \frac{\partial z_{q,p}}{\partial \hat{y}_2^1} & \frac{\partial z_{q,p}}{\partial \hat{x}_3^1} & \frac{\partial z_{q,p}}{\partial \hat{y}_3^1} & \frac{\partial z_{q,p}}{\partial \hat{x}_4^1} & \frac{\partial z_{q,p}}{\partial \hat{y}_4^1} & \frac{\partial z_{q,p}}{\partial \hat{x}_5^1} & \frac{\partial z_{q,p}}{\partial \hat{y}_5^1} & \frac{\partial z_{q,p}}{\partial \hat{x}_6^1} & \frac{\partial z_{q,p}}{\partial \hat{y}_6^1} \end{array} \right] \tag{77}$$

Suppose if the TDoA measurement is taken between motes N_1^1 and N_1^2, then $p = 1$ and $q = 2$,

$$H_{2,1} = \left[\begin{array}{cccccccccccc} \frac{\partial z_{2,1}}{\partial \hat{x}_1^1} & \frac{\partial z_{2,1}}{\partial \hat{y}_1^1} & \frac{\partial z_{2,1}}{\partial \hat{x}_2^1} & \frac{\partial z_{2,1}}{\partial \hat{y}_2^1} & \frac{\partial z_{2,1}}{\partial \hat{x}_3^1} & \frac{\partial z_{2,1}}{\partial \hat{y}_3^1} & \frac{\partial z_{2,1}}{\partial \hat{x}_4^1} & \frac{\partial z_{2,1}}{\partial \hat{y}_4^1} & \frac{\partial z_{2,1}}{\partial \hat{x}_5^1} & \frac{\partial z_{2,1}}{\partial \hat{y}_5^1} & \frac{\partial z_{2,1}}{\partial \hat{x}_6^1} & \frac{\partial z_{2,1}}{\partial \hat{y}_6^1} \end{array} \right] \tag{78}$$

where,

$$\frac{\partial z_{2,1}}{\partial \hat{x}_1^1} = \frac{\partial \sqrt{(\hat{x}_2^1 - \hat{x}_1^1)^2 + (\hat{y}_2^1 - \hat{y}_1^1)^2}}{\partial \hat{x}_1^1} = \frac{-(\hat{x}_2^1 - \hat{x}_1^1)}{\sqrt{(\hat{x}_2^1 - \hat{x}_1^1)^2 + (\hat{y}_2^1 - \hat{y}_1^1)^2}} \tag{79}$$

$$\frac{\partial z_{2,1}}{\partial \hat{y}_1^1} = \frac{\partial \sqrt{(\hat{x}_2^1 - \hat{x}_1^1)^2 + (\hat{y}_2^1 - \hat{y}_1^1)^2}}{\partial \hat{y}_1^1} = \frac{-(\hat{y}_2^1 - \hat{y}_1^1)}{\sqrt{(\hat{x}_2^1 - \hat{x}_1^1)^2 + (\hat{y}_2^1 - \hat{y}_1^1)^2}} \tag{80}$$

$$\frac{\partial z_{2,1}}{\partial \hat{x}_2^1} = \frac{\partial \sqrt{(\hat{x}_2^1 - \hat{x}_1^1)^2 + (\hat{y}_2^1 - \hat{y}_1^1)^2}}{\partial \hat{x}_2^1} = \frac{+(\hat{x}_2^1 - \hat{x}_1^1)}{\sqrt{(\hat{x}_2^1 - \hat{x}_1^1)^2 + (\hat{y}_2^1 - \hat{y}_1^1)^2}} \tag{81}$$

$$\frac{\partial z_{2,1}}{\partial \hat{y}_2^1} = \frac{\partial \sqrt{(\hat{x}_2^1 - \hat{x}_1^1)^2 + (\hat{y}_2^1 - \hat{y}_1^1)^2}}{\partial \hat{y}_2^1} = \frac{+(\hat{y}_2^1 - \hat{y}_1^1)}{\sqrt{(\hat{x}_2^1 - \hat{x}_1^1)^2 + (\hat{y}_2^1 - \hat{y}_1^1)^2}} \tag{82}$$

and,

$$\frac{\partial z_{2,1}}{\partial \hat{x}_3^1} = \frac{\partial z_{2,1}}{\partial \hat{y}_3^1} = \frac{\partial z_{2,1}}{\partial \hat{x}_4^1} = \frac{\partial z_{2,1}}{\partial \hat{y}_4^1} = \frac{\partial z_{2,1}}{\partial \hat{x}_5^1} = \frac{\partial z_{2,1}}{\partial \hat{y}_5^1} = \frac{\partial z_{2,1}}{\partial \hat{x}_6^1} = \frac{\partial z_{2,1}}{\partial \hat{y}_6^1} \tag{83}$$

Equations(78) to (83), gives

$$H_{2,1} = \begin{bmatrix} \frac{-(\hat{x}_2^1 - \hat{x}_1^1)}{\sqrt{(\hat{x}_2^1 - \hat{x}_1^1)^2 + (\hat{y}_2^1 - \hat{y}_1^1)^2}} & \frac{-(\hat{y}_2^1 - \hat{y}_1^1)}{\sqrt{(\hat{x}_2^1 - \hat{x}_1^1)^2 + (\hat{y}_2^1 - \hat{y}_1^1)^2}} & \frac{+(\hat{x}_2^1 - \hat{x}_1^1)}{\sqrt{(\hat{x}_2^1 - \hat{x}_1^1)^2 + (\hat{y}_2^1 - \hat{y}_1^1)^2}} & \frac{+(\hat{x}_2^1 - \hat{x}_1^1)}{\sqrt{(\hat{x}_2^1 - \hat{x}_1^1)^2 + (\hat{y}_2^1 - \hat{y}_1^1)^2}} & 0 & 0 & 0 & 0 \end{bmatrix} \tag{84}$$

Equation (84) gives the formulation for the H matrix when the TDoA measurement is taken between network

4.4.6 The parameter Q and R

The parameter Q represents the process noise covariance. In this project as the motes are stationary and no robot is used for mapping, the value of Q is assigned as a zero value. The parameter R is the measurement error covariance and is measured prior to the actual operation of the EKF technique. The measurement error covariance R is generally measured by taking some off-line sample measurements and then determining the variance of the measurement noise [24]. The value of R obtained through field experiments, yielded $\sigma = 0.02/3 = 0.00666667$.

4.5 Chapter Summary

In summary this chapter gives a detail description for the layout of the cricket mote, in order to achieve the self-calibration of the cricket motes. The step-by-step mathematical formulation for phase1 and phase2 provides a deep insight into the proposed algorithm.

5 Experimental Results

In this chapter, the experimental results obtained by simulating the proposed algorithm in MATLAB are discussed. Using the data provided by the field experiments, phase 1 of the proposed algorithm is implemented to get the rough estimates for the position of each mote.

The 'rectangular box' in figure 36 shows the outline of the field and the points

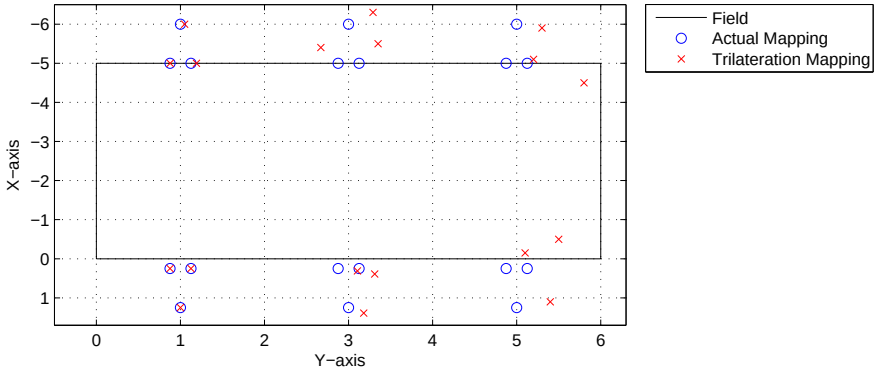

Figure 36: Localization using trilateration technique.

marked with 'circles' are the actual position of the motes. Points marked with 'cross' represents the localization of the motes obtained using the method of trilateration. It can seen from this figure that the error is large (within 2 m) mainly due to the faulty distance measurements. The error in localization of network N_1 and N_2 is very low because the distance measurements obtained have high accuracy. The error in localization of the cricket motes increases as the localization process moves towards the final network. To overcome this faulty localization problem, phase 2 of the algorithm is implemented. Figure 37 shows the scenario when phase 2 is implemented, considering only motes N_i^1 of each network (where, $i = 1, 2, ..., 6$). As seen in figure 37, motes N_1^1 and N_2^1 are localized almost accurately, while there is some error (less than 0.5 m) for other motes.

Figure 38 shows the RMS error values for localization of the motes. The RMS er-

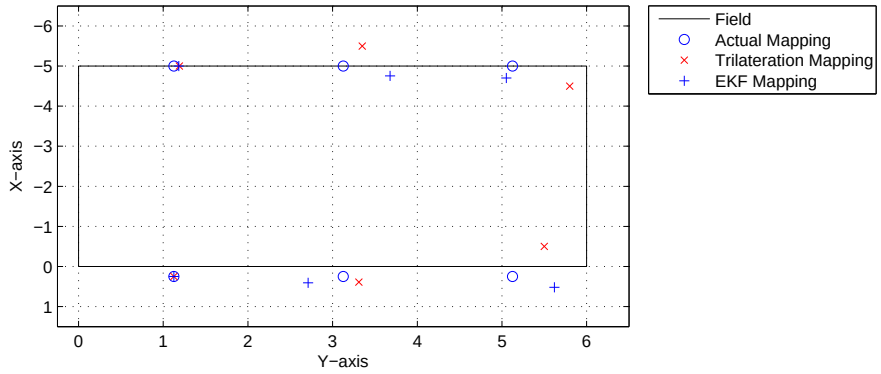

Figure 37: Correction in localization using EKF technique.

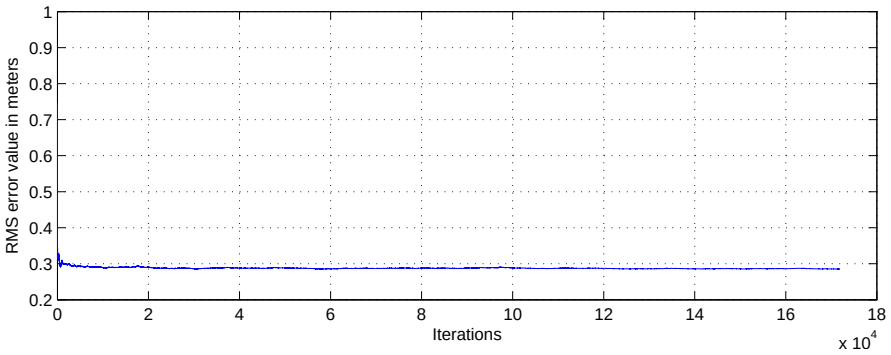

Figure 38: RMS error value in localization of the motes at each iteration.

ror value starts to decrease rapidly after a few iterations and then starts to decrease slowly. The RMS error value remains constant between 0.30 m and 0.27 m. It means that the state values estimated using the EKF technique never converges to its true state values. This is mainly due to the state observability issue i.e. maximum possible inter-mote distances or measurements are not obtained to observe the relationship between the states (position of the motes). As the relation between all state is not observed, the estimated position of the motes never converges to its actual values.

Now, assuming that the cricket motes are attached with omni-directional US transmitters and receivers, so that each mote can obtain distance measurements from adjacent motes. Phase 2 is re-implemented assumming that the distance measurements from the adjacent motes can be obtained.

Figure 39 shows the scenario when the motes are assumed to be omni-directional

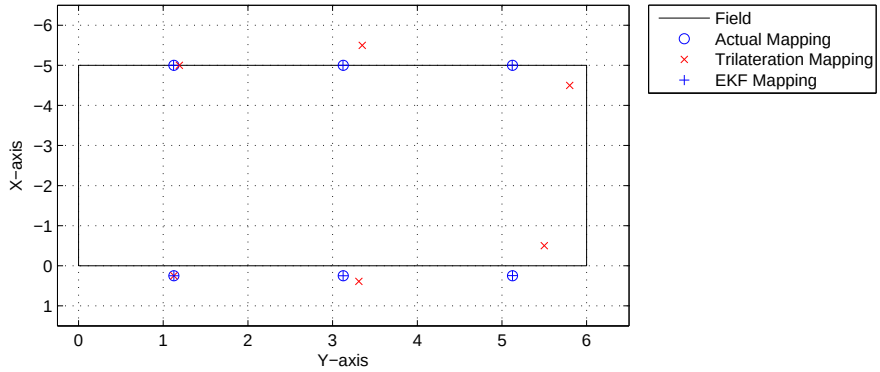

Figure 39: Localization with low RMS error value in case of increased measurements.

and are able to obtain distance measurements from adjacent motes. Due to increased in the number of the distance measurements, the localization of the motes has high accuracy and the estimated values of the motes position converges to their actual values.

Figure 40 shows the localization of the motes, with a RMS error value of less than

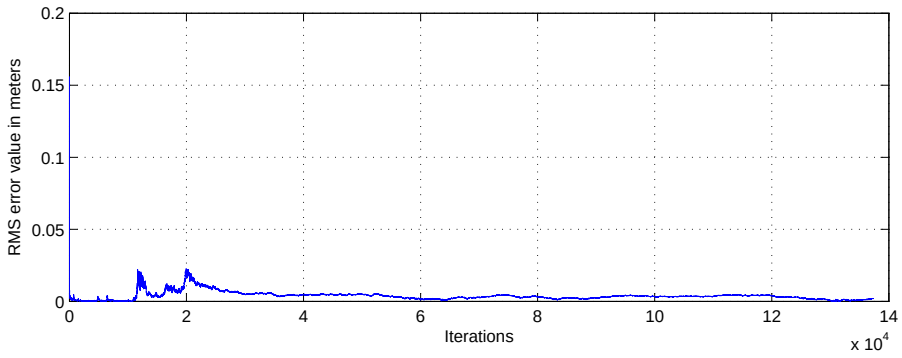

Figure 40: Localization with low RMS error value in case of increased measurements.

5 mm, when the number of distance measurements are increased. Therefore, with increase in the number of measurements, the observability of the states increases and motes are localized with high level of accuracy.

6 Conclusion and Future Work

This thesis presents a novel technique for self-calibration of the cricket motes. The intention for designing self-calibrating cricket motes is to find an easy solution for indoor localization and navigation of autonomous robotic systems. The following sub-sections summarizes the conclusions of this thesis work and further improvements.

6.1 Conclusion

This research work mainly focuses on the algorithm for self-calibration of the cricket motes. Once the cricket motes are localized themselves, they can provide localization services to multiple robots simultaneously.

Based on the literature survey, the current state of various localization schemes and the limitations of these schemes are discussed. By analyzing the working principle for each localization system, some limitations are identified. Based on the advantages provided by the cricket motes over the other localization systems, cricket location-aware system is chosen in this thesis to provide indoor localization. The localization technique applied by cricket motes is analyzed and discussed. Furthermore, the construction and working principle for the ultrasonic sensors of the cricket motes is described to understand the behavior of the US pulse generated by the cricket mote. Various field-experiment data is provided to understand the accuracy level achieved for a particular beacon-listener layout.

After carefully studying the accuracy zone of a given beacon-listener layout, the algorithm for self-calibration of the cricket motes is devised. Detail step-by-step formulation to the algorithm is discussed. A modified logic of SLAM algorithm is applied to get a good estimate for the position of the cricket motes placed at a particular lo-

cation.

Using the data from the field experiments, the proposed algorithm is implemented in a simulated environment using the MATLAB platform. The results obtained shows that the US sensors should have omni-directional ability for transmission and receiving the US pulse. This allows the cricket motes to localize with a high level of accuracy as compared to the cricket motes without omni-directional US sensors.

6.2 Future Work

The main objective of this thesis is to devise a novel technique for self-calibration of the cricket motes. As cricket motes are wireless sensor networks, the communication protocols for these wireless sensor networks are not discussed in this project. Future work should consist of implementing an efficient communication protocols for the cricket motes.

It should be noted that the maximum breadth of the field, for which the cricket motes can perform self-calibration is 5 m. Thus, the algorithm fails for fields with larger dimensions. Increasing the operating range for the cricket motes can solve this problem.

Localization of the cricket motes with low RMS error value can only be obtained if large number of inter-mote distance measurements are available. Due to non omni-directionality of the cricket motes US sensors, only few inter-mote distance measurements can be obtained; hence accurate localization cannot be obtained. Also, the total number of motes used for self-localization are 20, which is still a high number.

Cricket mote cost around $20 non-commercially. Addition of extra US sensors (to make the US transmitter and receiver omnidirectional) will cost the whole unit to be less than $40. Making an omnidirectional US sensor will solve the state observability issue and will result in precise mapping. Also the range of the given US sensor can be increased up to 16 meters, which will provide mapping for larger areas. The algorithm can be easily extended to 3D localization.

7 References

1. Trimble Navigation Limited http://www.trimble.com/

2. Introduction to GPS - Rutgers http://ocean.rutgers.edu/courses/gps/land_1_files /frame.htm

3. United States Naval Observatory (USNO) GPS Timing Data & Information http://tycho.usno.navy.mil/gps_datafiles.html

4. GPS Fundamentals http://www.wmccat.com/products/constTechGPS.jsp

5. GPS Overview - University of Colorado http://www.colorado.edu/geography /gcraft/notes/gps/gps_ftoc.html

6. Sonitor Technologies http://www.sonitor.com/technology

7. Ubisense Technologies http://www.ubisense.net/

8. Firefly User Guide - Gesture Central http://www.gesturecentral.com /firefly/FireflyUserGuide.pdf

9. J. Hightower and G. Borriello, A survey and taxonomy of location sensing systems for ubiquitous computing, CSE 01-08-03, University of Washington, Department of Computer Science and Engineering, Seattle, WA (August 2001)

10. R. Want, A. Hopper, V. Falcao, and J. Gibbons, The Active Badge Location System, *ACM Trans. Information Systems*, vol. 10, no. 1, pp. 91-102, Jan. 1992

11. N. Priyantha, A. Chakraborty, and H. Balakrishnan. The Cricket Location-Support System.*In Proc. 6th ACM MOBICOM Conf.*, pages 3243, Boston,MA, August 2000.

12. The Cricket Indoor Location System: An NMS project @ CSAIL MIT
http://cricket.csail.mit.edu/

13. A. Savvides, M. Srivastava, L. Girod, and D. Estrin, , C. R. Raghavendra, K. M. Sivalingam, and T. Znati, Eds., Localization in sensor networks, in *Wireless Sensor Networks*. Norwell, MA: Kluwer Academic, 2004.

14. Trilatertion basic http://en.wikipedia.org/wiki/Trilateration

15. T. Eren, D. Goldenberg,W. Whitley, Y. Yang, S. Morse, B. Anderson, and P. Belhumeur. Rigidity, computation, and randomization of network localization. In *Proc. 23rd Annual Joint Conference of the IEEE Computer and Communications Societies (INFOCOM'04)*, volume 4, pages 2673-2684, March 2004.

16. N. Priyantha, H. Balakrishnan, E. Demaine, and S. Teller, Mobile-Assisted Localization in Wireless Sensor Networks,*Proc. IEEE INFOCOM '05*, Apr. 2005.

17. N.B. Priyantha, H. Balakrishnan, E. Demaine, and S. Teller, Anchor-Free Distributed Localization in Sensor Networks,*Proc. First ACM Int'l Conf. Embedded Networked Sensor Systems (SenSys)*, 2003

18. D. Moore, J. Leonard, D. Rus, and S. Teller, Robust Distributed Network Localization with Noisy Range Measurements,*Proc. Second ACM Conf. Embedded Networked Sensor Systems (SenSys)*, Nov. 2004.

19. N Priyantha., The Cricket Indoor Location System, *PhD Thesis, Massachusetts Institute of Technology*, June 2005.

20. Introduction to Ultrasoundhttp://www.ndt-ed.org/
EducationResources/CommunityCollege/Ultrasonics/cc_ut_index.htm

21. Law-of-Cosine basic http://en.wikipedia.org/wiki/Law_of_cosines

22. H. Durrant-Whyte and T. Bailey, Simultaneous localisation and mapping (SLAM): Part I: The essential algorithms, *IEEE Robot. Autom. Mag.*,vol. 13, no. 2, pp. 99-110, Jun. 2006.

23. S Riisgaard, M R Blas. SLAM for Dummies: A tutorial approach for Simultaneous Localization and Mapping.

24. Bishop, G., Welch, G., An introduction to the Kalman Filter,*Course 8, Presented at ACM SIGGRAPH* (2001).

25. Kalman Filter basic http://en.wikipedia.org/wiki/Kalman_filter

26. Automated Guided Vehicle basic http://en.wikipedia.org/wiki/Automated_guided_vehicle